CHARACTERIZATION OF THE SURFACTIN AND FENGYCIN-INDUCED MECHANISMS INVOLVED IN THE PROTECTION OF DICOTYLEDONS

DEMORTIER THOMAS

TRAVAIL DE FIN D'ETUDES PRESENTE EN VUE DE L'OBTENTION DU DIPLOME DE MASTER BIOINGENIEUR EN CHIMIE ET BIO-INDUSTRIES

ANNEE ACADEMIQUE 2022-2023

CO-PROMOTEURS: DELEU MAGALI ET DE CLERCK CAROLINE

[1]l'autorité académique est représentée par les promoteurs membre du personnel enseignant de GxABT

CHARACTERIZATION OF THE SURFACTIN AND FENGYCIN-INDUCED MECHANISMS INVOLVED IN THE PROTECTION OF DICOTYLEDONS

DEMORTIER THOMAS

TRAVAIL DE FIN D'ETUDES PRESENTE EN VUE DE L'OBTENTION DU DIPLOME DE MASTER BIOINGENIEUR EN CHIMIE ET BIO-INDUSTRIES

ANNEE ACADEMIQUE 2022-2023

CO-PROMOTEURS: DELEU MAGALI ET DE CLERCK CAROLINE

Acknowledgments

Abstract

Surfactin (srf) and fengycin (fgc) are two of the cyclic lipopeptides (CLPs) produced by beneficial bacteria of the *Bacillus* genus. In the context of studying the biocontrol activity of these bacteria, the role of the two CLPs was investigated in this work. Literature mentions direct (pathogen antagonism) and indirect (plant defense elicitation) plant protection effect for these molecules. In this study, we first investigated their direct effect against fungal pathogens. While they are both known to be effective against various pathogens, only fgc, and not srf, displayed antifungal properties against *Botrytis cinerea*. Their effect on spore germination should, however, be further investigated. Then, their indirect effect was studied through quantification of early plant defense events such as calcium influx, Reactive Oxygen Species (ROS) production and extracellular medium alkalinization on *Arabidopsis thaliana* root protoplasts. Their effect was compared to those of chitin (cht) and flagellin (flg), two molecules of pathogenic origin able to elicit Pattern Triggered Immunity (PTI), a well-studied plant defense mechanism. No significant response could be observed after fgc treatments at concentrations between 2.5µM and 20µM. Srf, on the other hand, triggered calcium fluxes and ROS production. The results allowed to observe that srf does trigger early defense responses, but not in the same way as PTI elicitors. In addition, we observed that srf decreases the fluidity of the plant plasma membrane, supporting the hypothesis that the srf-membrane interaction may activate mechanosensitive ion channels, triggering early immune events.

Key words: Surfactin, Fengycin, Induced Systemic Resistance (ISR), Plasma membrane, Lipopeptides.

Résumé

La surfactine (srf) et la fengycine (fgc) sont deux des lipopeptides cycliques (LPCs) produits par des bactéries bénéfiques du genre Bacillus. Dans le cadre de l'étude de l'activité de biocontrôle de ces bactéries, le rôle des deux LPCs a été étudié dans ce travail. La littérature mentionne des méchanismes de protection des plantes directs (antagonisme avec les pathogènes) et indirects (stimulation de la défense des plantes) pour ces molécules. Dans cette étude, nous avons d'abord étudié leur effet direct contre les pathogènes fongiques. Bien qu'elles soient toutes deux connues pour leur efficacité contre divers pathogènes, seule la fgc, et non la srf, a montré des propriétés antifongiques contre *Botrytis cinerea*. Leur effet sur la germination des spores devrait cependant être étudié de manière plus approfondie. Ensuite, leur effet indirect a été étudié par la mesure d'événements précoces de défense des plantes tels que l'influx de calcium, la production d'espèces réactives d'oxygène (ROS) et l'alcalinisation du milieu extracellulaire sur les protoplastes de racines d'*Arabidopsis thaliana*. Leurs effets ont été comparés à ceux de la chitine (cht) et de la flagelline (flg), deux molécules d'origine pathogène capables d'activer l'immunité déclenchée par des motifs (PTI), un mécanisme de défense des plantes bien étudié. Aucune réponse significative n'a pu être observée après des traitements à la fgc à des concentrations comprises entre 2,5µM et 20µM. La srf, par contre, a déclenché des flux de calcium et la production de ROS. Les résultats ont permis d'observer que la srf déclenche des réponses de défense précoces, mais pas de la même manière que les éliciteurs PTI. En outre, nous avons observé que le srf diminue la fluidité de la membrane plasmique de la plante, ce qui soutient l'hypothèse selon laquelle l'interaction srf-membrane peut activer des canaux ioniques mécanosensibles, déclenchant ainsi des événements immunitaires précoces.

Mots-clés: Surfactine, Fengycine, Résistance Systémique Induite (RSI), Membrane plasmique, Lipopeptides.

Abbreviations

Surfactin (srf), fengycin (fgc), chitin (cht), flagellin (flg), cyclic lipopeptide (CLP), pattern triggered immunity (PTI), generalized polarization (GP).

Table of contents

Introduction

Context

Pesticides are a common way to increase food production by regulating pests in the field (Popp et al., 2013). However, their abusive use has led to many drawbacks, such as toxicity towards non-target organisms (Serrão et al., 2022), water pollution (Srivastav, 2020), and multiple human health issues (Cocco, 2016; Sabarwal et al., 2018). An interesting alternative is the use of biocontrol agents that are less toxic to both the environment and humans (Kumar et al., 2021). Bacteria of the *Bacillus* genus are well-known biocontrol agents that were shown to be effective against diverse plant pathogens through the production of several metabolites (Fira et al., 2018). Among them, cyclic lipopeptides (CLPs) have particularly been studied for their involvement in biocontrol activity. This study focuses on two important families of CLPs: surfactin (srf) and fengycin (fgc).

Surfactin and fengycin

First discovered in 1968 in the culture broth of *B. subtilis* (Kakinuma, Sugino, et al., 1969), srf gets its name from its surfactant property. It has been shown to reduce surface tension of water from 72mN/m to 27 mN/m at low concentration (Arima et al., 1968). It was first described as a lipopeptide composed of a heptapeptide lactone ring linked to a 3-hydroxy-13-methyl-tetradecanoic acid with the peptide sequence L-Glu-L-Leu-D-Leu-L-Val-L-Asp-D-Leu-L-Leu (Fig. 1A)(Kakinuma, Ouchida, et al., 1969; Kakinuma, Sugino, et al., 1969). However, the term srf regroups multiple molecules (Peypoux et al., 1999), so the fatty acid can be 12-17 C long and in different configurations (Théatre et al., 2021) and the amino acid sequence can vary. When the term srf is used, it generally refers to molecules with the same peptide moiety as described by (Kakinuma, Sugino, et al., 1969). However, the amino acids (AA) in position 2, 4 and 7 can be replaced by other hydrophobic acids during the assembly. This variability in the peptide sequence is due to the ability of the enzymes responsible for srf production to recognize multiple amino acids (Galli et al., 1994; Théatre et al., 2021). The chiral sequence always remains LLDLLDL, whatever the AA present in the peptide (Bonmatin et al., 2003).

Fgc is another CLP produced by species of the *Bacillus* genus. When discovered in 1986, it was directly described as a group of similar variants such as srf (Vanittanakom et al., 1986). The main components are named fengycin A and B. They are formed of a decapeptide with cyclization between the 3rd and 10th AA (Samel et al., 2006) linked to an alkyl chain that can be saturated or not with a length of 14C-18C (Ongena et al., 2005). Their AA chains are L-Glu-D-Orn-D-Tyr-D-Thr-L-Glu-D-Ala-L-Pro-L-Gln-L-Tyr-L-Ile for fgc A and the D-Ala is replaced by D-Val in the sequence of fgc B (Fig. 1B)(Schneider et al., 1999).
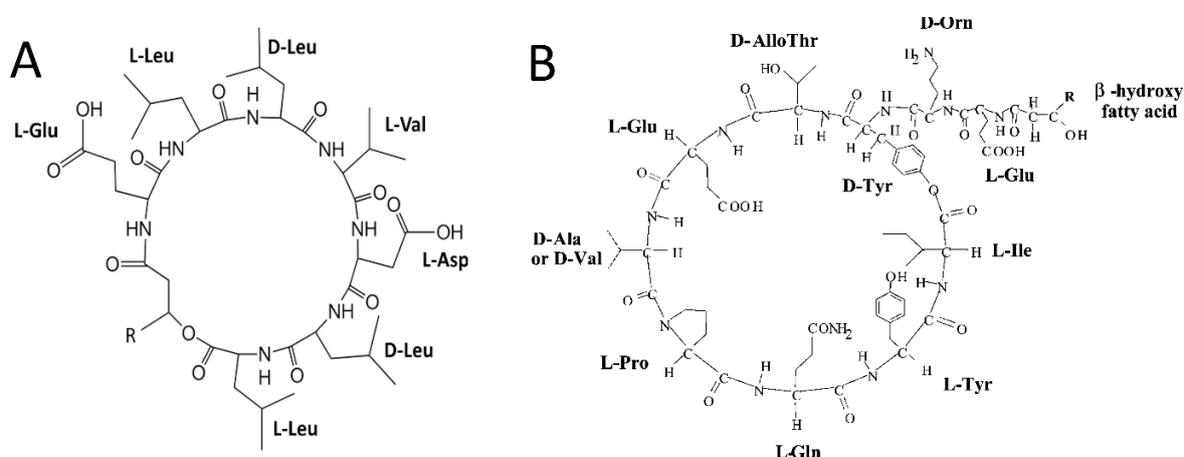
Figure 1 [A] Surfactin as described by Kakinuma, Ouchida, et al., 1969, R is the 3-hydroxy-13-methyl-tetradecanoic acid. [B] Fengycin A and B, R is the alkyl chain of length 14C-18C.

Bacillus as a biocontrol agent

The biocontrol activity of *Bacillus* is based on three main actions: colonization of the rhizosphere, direct antagonistic activity against pathogens and stimulation of the plant's defense mechanisms. The production of secondary metabolites such as CLPs may have a role in these actions.

Rhizosphere colonization

Beneficial bacteria form biofilms on the host roots (Ramey et al., 2004), providing resistance against pathogens through competition for niches and nutrients (Kamilova et al., 2005). When genes associated to the biofilm production are inhibited, the biocontrol activity decreases (Chen et al., 2013). The role of srf has been studied in the formation of this biofilm. It has been shown that its surface activity (Leclère et al., 2006) increases *Bacillus* motility (Kinsinger et al., 2003). Through srf production, colonization of the rhizosphere by *Bacillus* is increased, competing with pathogens in the rhizosphere and thus reducing their impact on the plant (Bais et al., 2004; Pandin et al., 2017).

Direct antagonism

Since *Bacillus* has been shown to have an antagonistic effect on multiple pathogens (Caulier et al., 2018; Lertcanawanichakul & Sawangnop, 2008), the role of its metabolites has been studied. Concerning srf, its antiviral properties have been established (Kracht et al., 1999). However, its efficiency to control fungal (G A et al., 2013; Krishnan et al., 2019; Meena et al., 2020; Ongena & Jacques, 2008) and bacterial (Bais et al., 2004; Lilge et al., 2022) pathogens is controversial and deserves to be studied more in detail. Fgc is particularly known for its antifungal activity, which has first been discovered against *Paecilomyces varioti* (Vanittanakom et al., 1986). This antifungal activity is considered to be the caused by fungi membrane permeabilization (Patel et al., 2011; Vanittanakom et al., 1986).

Plant defense mechanisms

Plants are able to defend themselves against pathogens through pattern triggered immunity (PTI) (Fig. 2). This immune response is started by the perception of elicitors or damage-associated molecular patterns (DAMPs) by pattern recognition receptors (PRRs) (Janeway & Medzhitov, 2002; Matzinger, 2002). Elicitors are extrinsic molecules containing pathogen- or microbe-associated molecular patterns (PAMPs and MAMPs) that are also perceived by PRRs (Boller & Felix, 2009). Those patterns are conserved molecular structure commonly found in a vast array of pathogens, such as fungi, bacteria and viruses. PRR are transmembrane receptor kinases (RKs) or receptor proteins (RPs) composed of multiple domains. The extracellular domain (ECD) is often composed of leucine-rich repeats (LRRs) that perceive part of the elicitor. This provokes a conformational change in the transmembrane domain, often made of a unique helix that anchors the receptor in the cellular membrane. This modification transfers the signal inside the cell to either a cytosolic kinase or to a short tail depending on the receptor's nature. Studied PRRs are often bonded to a co-receptor of LRR-RK nature that participate in cytosolic phosphorylation cascade. The kinase activity triggers a reaction cascade inside the cell that leads to the immune response. Though research has already been conducted on the metabolic pathway triggering immunity, information is still lacking to fully understand its functioning (DeFalco & Zipfel, 2021). Multiple phenomena take place following pattern recognition. Together, they compose the immune response of PTI. Most studies report an increase in cytosolic calcium ions ($[Ca^{2+}]cyt$), ion fluxes through the membrane, mainly K^+, Cl^- and H^+ (the former leading to extracellular alkalinization), apoplastic reactive oxygen species (ROS) production by the RBOHD enzyme and expression of PTI-associated genes (Yu et al., 2017).
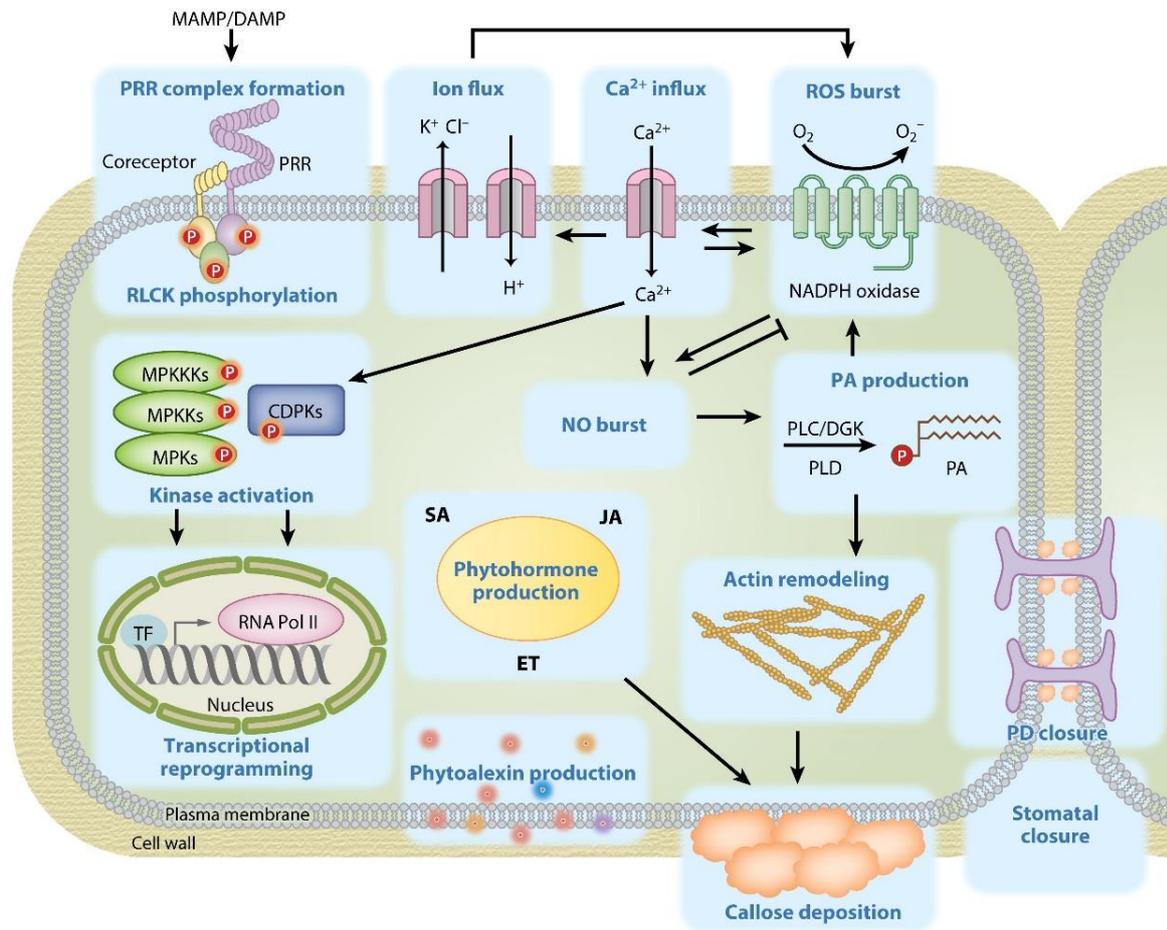
Figure 2 Pattern Triggered Immunity (PTI) response after the elicitor perception by the plant cells (Yu et al., 2017).

Flagellin (Flg) and chitin (cht) are two well-studied PTI elicitors of pathogenic origin. Flg is the main component of bacterial flagellum, making it an indicator to plants of the presence of bacterial pathogens (Hajam et al., 2017). The epitope flg22 is the PAMP recognized by the LRR-RKs FLAGELLIN-SENSING 2 (FLS2) (Gómez-Gómez & Boller, 2000). FLS2 is associated to a somatic embryogenesis receptor kinase (SERK) co-receptor, the BRI1 associated kinase 1 (BAK1, also referred to as SERK3) for downstream signaling (Chinchilla et al., 2007; Roux et al., 2011). Cht is, after cellulose, the most abundant polysaccharide. It can be found in a vast array of organisms such as fungi, insects, mollusks and nematodes but also in algae and protists (Merzendorfer, 2011). As the main component of the cell wall of fungi, it is a MAMP of interest while studying antifungal immunity. In *Arabidopsis*, cht is recognized via a complex formed by a lysin motif RK named cht elicitor receptor kinase 1 (CERK1) and LysM-containing receptor-like kinase 5 (LIK5) (Cao et al., 2014).

Srf extracts have been shown to elicit induced systemic resistance (ISR) in dicotyledons (Henry et al., 2011; Ongena et al., 2007) but no known PRR has been associated to the molecule detection so far (Jourdan et al., 2009; Ongena & Jacques, 2008). Furthermore, when digesting PRR from cells using protease, srf activity has not been reported to be affected (Henry et al., 2011). Plant immunity is also activated by a micromolar concentration of this lipopeptide, whereas nanomolar PAMPs solutions are sufficient to trigger it (Jourdan et al., 2009; Tran et al., 2007). The activation of early defense mechanism is thus suspected to rely on a distinct mechanism than PTI (Henry et al., 2011; Pršić & Ongena, 2020).

Plant plasma membrane

The plasma membrane (PM) is the physical barrier between the cytoplasm and the exterior of a cell. Its main functions are to transport various solutes in and out of the cell, as well as perceive and transmit signals (Sussman & Harper, 1989). PM is a lipid bilayer containing proteins and carbohydrates (Fig. 3). The three main types of lipids composing PM are: glycerolipids (mainly phospholipids), sterols and sphingolipids (Furt et al., 2011). Lipids are not distributed evenly throughout the membrane. The general composition of each leaflet differs (Tjellström et al., 2010) and it is also laterally heterogenous (Varma & Mayor, 1998). The main hypothesis of PM organization is the presence of "rafts" or micro-/nano-domains in the fluid membrane. Those rafts are made of sphingolipids and cholesterol (Goñi, 2019). Srf is able to interact with membrane lipids (Gilliard et al., 2022) and this interaction can affect membrane fluidity and organization in cancer cells (Wójtowicz et al., 2021). However, its affinity for the membrane depends on various factors, such as its alkyl chain length and the composition of the membrane. The srf-PM interaction increases with the chain length and in the presence of solid ordered lipid phases in the membrane (Henry et al., 2011).
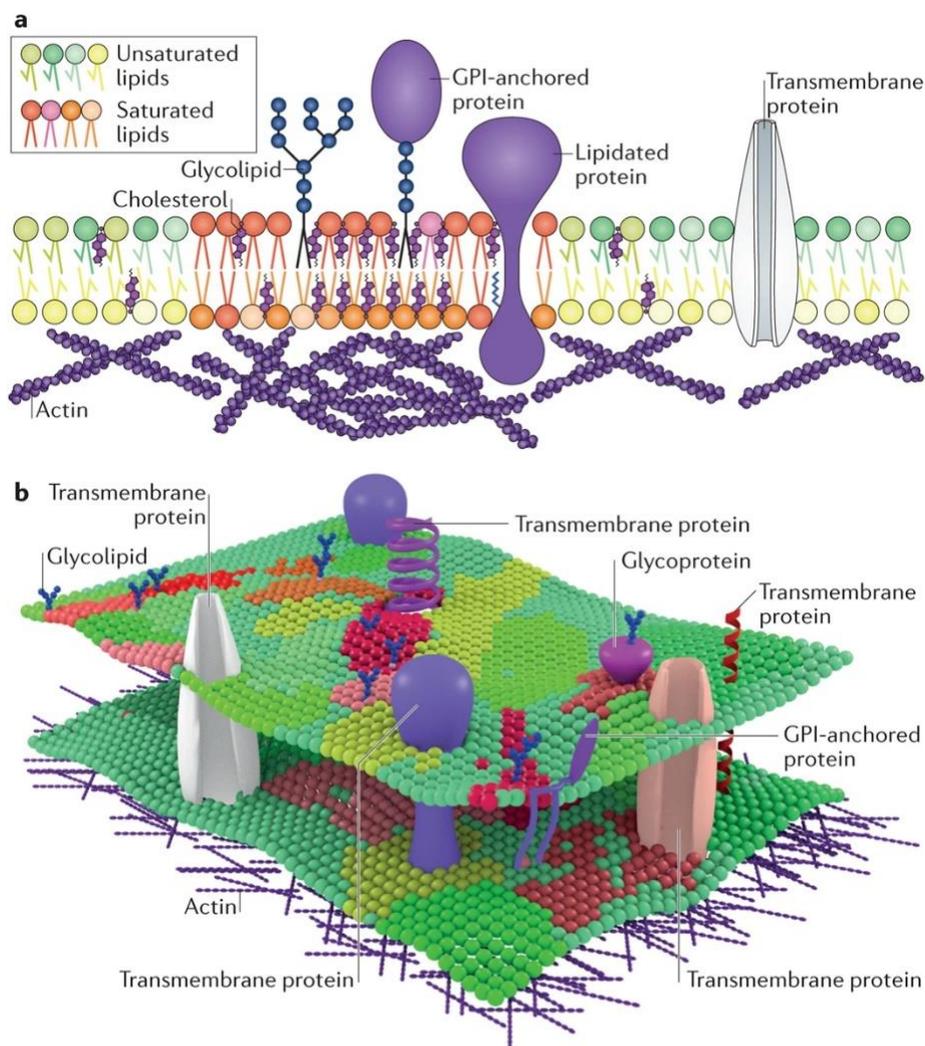
Figure 3 Organization of the plasma membrane in 2D [A] and 3D [B] (Sezgin et al., 2017).

Knowing this, the interaction of srf with sphingolipid-enriched microdomains of the membrane is suspected to be the start of the immune response but other hypothesis such as low-affinity receptors cannot be ruled out (Henry et al., 2011; Pršić & Ongena, 2020).

Objectives and strategy

The goal of this study is to characterize the mechanisms by which srf and fgc lead to the protection of dicotyledons against fungal pathogens. While fgc is mainly known for its direct effect on fungal pathogens (Vanittanakom et al., 1986), srf has shown its potential role as a plant defense elicitor (Ongena et al., 2007). However, the detailed mechanism at the molecular level is far from understood. The role of the two lipopeptides in both direct and indirect plant protection was thus investigated in this work. In order to understand the mechanisms through which they lead to protection of dicotyledons, *Arabidopsis thaliana* has been selected as a plant model. *A. thaliana* is the most studied flowering plant, with more than 5000 publications on PubMed each year (http://www.ncbi.nlm.nih.gov/pubmed). It drew scientific interest due to its convenience to manipulate and because it was, together with rice, one of the first plants with a fully sequenced genome, allowing easy access to mutant strains (Koornneef & Meinke, 2010; Pruitt et al., 2003). Other advantages of this species are its size, easy and significant seed production, and rapid life cycle (Koornneef & Meinke, 2010).

Direct effect of srf and fgc on pathogens

The first objective of this study is to evaluate the direct effect of srf and fgc on fungal pathogens. Fgc is known for its effect on fungi (Vanittanakom et al., 1986). To evaluate if similar properties apply to srf, *Botrytis cinerea* was used as a model. *B. cinerea* is a necrotrophic fungus that is known to cause the gray mold disease in more than 200 crops worldwide (Williamson et al., 2007). It is considered to be one of the most important fungal pathogens both scientifically and economically, making it an extensive source of research concerning dicotyledonous hosts (Dean et al., 2012). Two potential effects have been measured: the inhibition of the spore germination and the impact on mycelial growth of already germinated specimens. Some molecules, such as essential oils, have been observed to have a different impact on those two factors (De Clerck et al., 2020). Three srf concentrations (2.5, 10 and 20µM) have been selected to characterize if the response intensity is related to the concentration. Fgc was also tested with the same concentrations to verify its antifungal properties and compare them to the srf ones.

Indirect effect of srf and fgc on plant protection

The second objective was to compare the early defense mechanisms induced by CLPs and known PTI elicitors in dicotyledons. For this part, we used protoplast generated from *Arabidopsis* roots by digesting the cell wall of plant cells in order to have a direct access to the plasma membrane (Gilliard et al., 2021). However, protoplasts are able to regenerate their cell wall within days (Yokoyama et al., 2016). Thus, the effect of the cell wall on the response to the different treatments can also be characterized if we consider the freshly isolated protoplasts (deprived of their cell wall, also referred to as "fresh protoplasts") and the 1-day-old protoplasts (with a partial regeneration of their cell wall) (Annex 1).

The first early defense mechanism that was studied was the Ca^{2+} influx (Köster et al., 2022). Two methods have been used to measure the internal (cytosolic) Ca^{2+} concentrations. The first uses a fluorescent probe called Fluo-4 AM that emits light when chelating calcium cations. This probe inserts itself inside protoplasts and not in the surrounding medium to assess cytosolic Ca^{2+} concentrations (Qiu et al., 2020). The other method uses *A. thaliana* genetically modified to produce an enzyme called aequorin inside its cells. Aequorin is capable of transforming the luciferin coelenterazine into an excited coelenteramide molecule. When coelenteramide relaxes, it emits a 469nm light. The speed of the aequorin enzyme activity, measured by the production of luminescence, is related to the concentration of Ca^{2+} around it (Kanchiswamy et al., 2014). Thanks to an R code, it is possible to relate light emission intensity to the calcium content inside the protoplasts (Ranf et al., 2012).

The second early defense mechanism studied was ROS production (Waszczak et al., 2018). As observed by Henry et al. 2011, intracellular ROS production happens before the extracellular. The probe DCFH-DA was thus used to quantify [ROS]$_{intra}$ on fresh and 1-day-old protoplasts.

Other early defense events considered were the extracellular medium alkalinization (Gerber et al., 2004) and change in conductivity due to more ion exchange (Falhof et al., 2016). Those responses were measured around the roots of whole plants to mimic naturally occurring phenomena. The measurements were done thanks to a pH microprobe and a compact conductivity meter.

Interaction with the plasma membrane

The third objective was to compare the effect of srf, fgc, cht and flg on the plasma membrane fluidity. This objective was set in order to explore the hypothesis that the interaction of srf with the plasma membrane is the start of the induced resistance. The fluorescent probe laurdan, a well-known probe for fluidity assessment (Amaro et al., 2017), was used. Di-4-ANEPPDHQ is another fluorescent probe that has been used in previous studies in plants (Gronnier et al., 2017; Sandor et al., 2016). In order to compare the results, and because laurdan and di-4-ANEPPDHQ may not react in the same way (Amaro et al., 2017), both probes have been used in the experiments. All tests have been performed on both fresh and 1-day-old protoplasts in order to study the influence of the cell wall on membrane fluidity and its impact on the response.

Material and method

Biological material

The strain of *B. cinerea* used in the experiment was the isolate R16, that resulted from the cross SAS56 x SAS405 (Faretra & Pollastro, 1991), provided by the Microbial Processes and Interactions Laboratory (Terra Teaching and Research Center, Gembloux Agro-Bio Tech). The pathogen was stocked in glycerol at -80°C until needed for the experiments.

Srf and fgc used were both already purified fraction of a mix of naturally synthesized homologs provided by the Microbial Processes and Interactions Laboratory (Terra Teaching and Research Center, Gembloux Agro-Bio Tech).

Inhibition of mycelial growth measurements

B. cinerea was taken out of the stock and plated on PDA. The pathogen was then grown for 10 days in a chamber (23°C, 16D:8N photoperiod) before use in the experiment. Round Petri dishes (Ø 90mm) were filled with 35mL of sterilized Potato Dextrose Agar (PDA, Merck) containing 2.5, 10 or 20µM of either srf or fgc diluted in ethanol, or ethanol alone for the negative control. A 0.8mm wide mycelial plug of *B. cinerea* already grown for 10 days was placed in the center of each dish with the mycelium facing down. The sealed dishes were placed for 5 days in the same growing chamber. The radius of each fungus was measured every 24h. The Growth Inhibition factor (GI) was calculated at each time point as: $GI = \frac{Rc-R}{Rc}$ where Rc is the radius of the control and R is the radius of the treatment.

Inhibition of spore germination measurements

To prepare a spore suspension, *B. cinerea* was transplanted in PDA Petri dishes from the stock and then placed successively 4 days in the dark, 2 days in the light and then again in the dark in order to stimulate sporulation in the same growing chamber as described here above. The spores were then retrieved by scrapping them in sterile physiological water and filtering the suspension through a fine sterile muslin to retain medium and mycelium fragments. Spore suspension was then quantified using a Burker cell and adjusted to a 3.10^5 spores/mL concentration.

A first protocol was adapted from (De Clerck et al., 2020). After preparing the spore suspension as described above, Potato Dextrose Broth (PDB, Merck) was prepared as described by the supplier and autoclaved. In transparent 96-well microplates (Greiner Bio-One™ CellStar™, Fischer Scientific), the wells were filled with 50µL PDB, 50µL spore suspension and 50µL 3-fold concentrated treatment. The treatments applied were 2.5, 10 and 20µM of either srf or fgc final concentration. EtOH 0.1% was used for the control. Blank wells were filled by replacing the treatment with physiological water. The absorbance at 630nm (Abs 630) was measured every 12 hours for 36 hours using the Spark® microplate reader (Tecan) with constant shaking at 27°C.

A second protocol was tested by filling 15mL Falcon tubes with 6mL of one part PDB, one part spore suspension and one part 3-fold concentrated treatment. The tubes were stored horizontally on an agitator at room temperature for 72 hours. Abs 630 was measured every 24 hours using the Spark® microplate reader (Tecan).

Plant growth condition

Arabidopsis thaliana Columbia ecotype (Col-0) seeds were grown in vertically stored 120x120mm Petri dishes containing half-strength Murashighe and Skoog medium (M0222, Duchefa Biochimie) with addition of 1% (w/v) sucrose and 1 % (w/v) agar. The sealed dishes were stored at 23°C with a photoperiod of 12 hours and a light intensity of 100µmol s^{-1} m^{-2}. Seedlings were grown for 1 to 2 weeks depending of the following experiments.

Root protoplast isolation

The procedure was adapted from (Yoo, S.-D. *et al.* (2007), Evrard, A. *et al.* (2012)). For each experiment, 30mg of *A. thaliana* seeds were grown as detailed above. After 13-15 days, the roots were cleaned and cut into 1-2mm segments. The root fragments were then incubated for 3 hours in the dark at room temperature in 6mL of protoplasting solution (20 mM MES pH 5.7, 0.4 M mannitol, 20 mM KCl, 10 mM $CaCl_2$, 0.1 % (w/v) BSA, 1.5 % (w/v) cellulase R10, 0.4 % macerozyme R10). The incubated solution was filtrated on double-stacked gauze to separate the roots from the protoplast suspension. Protoplasts were then washed by centrifuging the filtrate and resuspending the pellet in 6mL of W5 solution (4mM MES pH 5.7, 154 mM NaCl, 125 mM $CaCl_2$, 5mM KCl). Washed protoplasts were resuspended in WI_{Ca} solution (2mM MES pH 5.7, 0.5 M mannitol, 20 mM KCl, 2mM CaCl2) at a final concentration between 10^5 and 2.10^5 protoplasts per mL.

Aequorin luminescence measurements

Coelenterazine-h (Promega) was added to a protoplast suspension of aequorin-producing *A. thaliana* mutant (Col-0^{AEQ}) cells at a 10µM final concentration. The solution is incubated for one hour in the dark at room temperature. Then, wells of a white 96-well microplates (LumiNunc ™, ThermoFischer) were filled with 100µL of the protoplast suspension. The luminescence was measured using Spark® microplate reader (Tecan) with an integration time of 300ms. Luminescence was first read every 6 seconds for 2 minutes to measure the resting levels. Afterwards, 25µL of 5-fold concentrated treatment was manually added to each well before directly reading the luminescence for 25 minutes. The remaining aequorin was discharged by adding 125µL of 2M $CaCl_2$ in each well and before recording for 4 minutes for normalization. To standardize measurements, data of each time point were processed as speed constant rate (L/Lmax) by dividing the luminescence measured at this time point by the sum of all the remaining luminescence of the well (see normalization above). This conversion in L/Lmax is used to take into account putative variability in coelenterazine or aequorin content between wells. Data processing was performed with FlagScreen R-script (Ranf, S. *et al. 2012)*. Treatments tested were srf 10µM, flg 1µM, cht 100µg/mL, fgc 2.5, 10 and 20µM and ethanol 0.1% (control), each at final concentration.

Calcium measurements with Fluo-4 AM

Fluo-4 AM (ThermoFischer) from a 5mM stock solution in DMSO was added to a protoplast suspension at 5µM final concentration. The suspension was incubated in the dark at room temperature for 1 hour before centrifugation at 850rcf for 6 minutes. The pelleted protoplasts were then resuspended in an equivalent volume of WI_{Ca} solution before incubating them for one more hour under the same conditions. Then wells of a black 96-well microplates (Greiner Bio-One™ CellStar™, Fischer Scientific) were filled with 100µL of protoplast suspension. The fluorescence was recorded using Spark® microplate reader (Tecan). Wavelengths were set at 465(±35)nm for excitation and 535(±25)nm for emission. Fluorescence was then read every 20 seconds for 2 minutes to measure resting levels. Then, 25µL of 5-fold concentrated treatment was manually added to each well before reading the fluorescence for 30 minutes. Data were processed as Normalized Fluorescence Increase, which was calculated as $\frac{F}{F_0}$, where F is the fluorescence at each time point and F_0 is the fluorescence at the first time point. Treatments tested were srf 10µM, flg 1µM, cht 100µg/mL, fgc 2.5, 10 and 20µM and ethanol 0.1% (control), each at final concentration.

Cytosolic ROS production measurements

DCFH-DA was added to a protoplast suspension at a 10µM final concentration and the suspension was incubated in the dark at room temperature for 15 minutes. Then wells of a black 96-well microplates (Greiner Bio-One™ CellStar™, Fischer Scientific) were filled with 100µL of protoplast suspension. The fluorescence was recorded using Spark® microplate reader (Tecan). Wavelengths were set at 465(±35)nm for excitation and 535(±25)nm for emission. Fluorescence was then read twice to measure resting levels.

Then, 25µL of 5-fold concentrated treatment was manually added to each well before reading the fluorescence every 2 minutes for 1 hour. Data were processed as Fluorescence Increase and Fold Increase. The first was calculated by subtracting the fluorescence at each time point (F) to the fluorescence at the first time point (F_0). The latter was defined for each well as the ratio between the fluorescence variation obtained at each time point in this well and the mean fluorescence variation obtained at the same time point in all wells treated with the control. Treatments tested were srf 10µM, flg 1µM, cht 100µg/mL, fgc 2.5, 10 and 20µM and ethanol 0.1% (control), each at final concentration.

Conductivity and pH variation of extracellular root medium measurements

Plants grown as already described were transferred in solution containing 0.1 mM KCl, 0.5 mM $CaCl_2$, 0.3 mM NaCl and 0.02 mM MES at pH 5.8 the day before the measurements. The day of the measurements, 4 plants with similar root size were placed in 12 well microplate with roots submerged in 6mL of the same solution containing either 10 µM of srf, 100µg/mL cht, 0.9% of Triton X-100 (trt) or control treatment (0.1% ethanol). The pH was measured with pH microprobe (In lab micro, METTLER TOLEDO) while the conductivity was measured using compact conductivity meter LAQUAtwin-EC-33 (HORIBA scientific) every 5 minutes for 40 minutes. The experiment was conducted 3 times in a row.

Laurdan polarization in protoplast membrane measurements

Freshly prepared Laurdan (3 mM stock solution in 100% ethanol) was added to a protoplast suspension at 3µM final concentration to be incubated in the dark at room temperature for 1 hour. The fluorescence was recorded using Spark® microplate reader (Tecan) with black 96-well microplates (Greiner Bio-One™ CellStar™, Fischer Scientific). Wavelengths were set to 360(±35)nm for excitation and 430(±20)nm and 485(±20)nm for emission. For each treatment, 2 wells were filled with 100µL of Laurdan-treated protoplast suspension each and a third with the same volume of untreated suspension. Fluorescence was then read twice to measure resting levels. Then, 25µL of 5-fold concentrated treatment was manually added to each 3 wells before reading the fluorescence every 2.5 minutes for 20 minutes. Data was processed as Generalized Polarization (GP) which was defined as GP = $\frac{(I_{430nm}-I_{485nm})}{(I_{430nm}+I_{485nm})}$, were I_{430nm} and I_{485nm} represents the blank-subtracted fluorescence intensities at emission wavelengths of 430 nm and 485 nm respectively. The variation of GP (ΔGP) was calculated by subtracting the mean of the two GP values before treatment to the GP calculated for each time point. Treatments tested were srf 10µM, flg 1µM, cht 100µg/mL, fgc 2.5, 10 and 20µM and ethanol 0.1% (control), each at final concentration.

Di-4-aneppdhq polarization in protoplast membrane measurements

Di-4-ANEPPDHQ (from a stock solution at 2.5 mM in ethanol) was added to a protoplast suspension at 2.5 µM final concentration and the suspension was incubated in the dark at room temperature for 15 minutes. The fluorescence was recorded using Spark® microplate reader (Tecan) with black 96-well microplates (Greiner Bio-One™ CellStar™, Fischer Scientific). Wavelengths were set to 465(±35)nm for excitation and 580(±20)nm and 680(±30)nm for emission. For each treatment, 2 wells were filled with 100µL of Di-4-ANEPPDHQ-treated protoplast suspension each and a third with the same volume of untreated suspension. Fluorescence was then read twice to measure resting levels. Then, 25µL of 5-fold concentrated treatment was manually added to each 3 wells before reading the fluorescence every 2.5 minutes for 20 minutes. Data was processed as Generalized Polarization (GP) which was defined as GP = $\frac{I_{580nm}-I_{680nm}}{I_{580nm}+I_{680\,nm}}$, where I_{580nm} and I_{680nm} represent the blank-subtracted fluorescence intensities at emission wavelengths of 580 nm and 680 nm respectively. The variation of GP (ΔGP) was calculated by subtracting the mean of the two GP values before treatment to the GP calculated for each time point. Treatments tested were srf 10µM, flg 1µM, cht 100µg/mL, fgc 2.5, 10 and 20µM and ethanol 0.1% (control), each at final concentration.

Results

Antifungal properties of srf and fgc

Effect of srf and fgc on the mycelial growth of *B. cinerea*

The biocontrol potential of surfactin (srf) and fengycin (fgc) was first evaluated in terms of direct antifungal properties. The first aspect of direct antifungal effect investigated was the inhibition of mycelial growth of *B. cinerea*. The effect of srf and fgc at different concentrations on the mycelial growth of *B. cinerea* was evaluated by measuring the diameter (Fig. 4A) of the pathogen growing on PDA (Annex 2). From these data, the growth inhibition factor (GI) was calculated to scale the effect of each modality (Fig. 4B). Throughout the 4 days of experiment, all srf treatments stayed close to the negative control. Media containing fgc displayed a diminished growth of the pathogen compared to the control. For both molecules, no effect of the concentration has been noticed. After 48h of experiment, statistical analysis showed two significantly different groups of treatments (Fig. 5A). The first containing control and srf treatment with a mean mycelial diameter of 3.25 cm and the second composed of the fgc treatments with a mean mycelial diameter of 1.52cm. GI values for fgc-treated mycelia reached around 0.48 after 24 hours and stayed constant while srf GI never increased. Over time, more deviation appeared but all trends remained. Hence, srf doesn't seem to have any effect on the mycelial growth of *B. cinerea*, while fgc reduced the growth by around 50%, independently of concentration used.
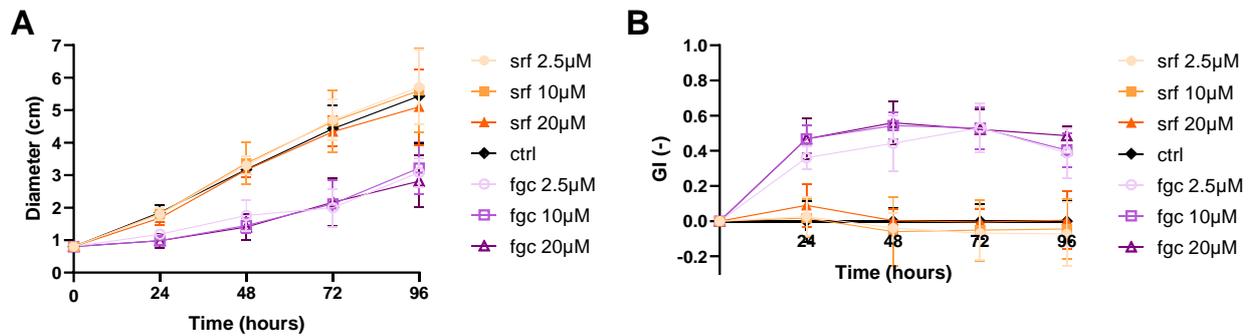
Figure 4 Measurement of surfactin and fengycin impact on B. cinerea *mycelial growth [A] Time-course evolution of* B. cinerea *mycelial growth on PDA treated with 2.5µM, 10µM and 20µM surfactin (srf) and 2.5µM, 10µM and 20µM fengycin (fgc) [B] Time-course evolution of the Growth Inhibition factor (GI) of* B. cinerea *in presence of 2.5µM, 10µM and 20µM srf or 2.5µM, 10µM and 20µM fgc. Data are shown as mean ± SD, n=6 from two independent triplicates.*
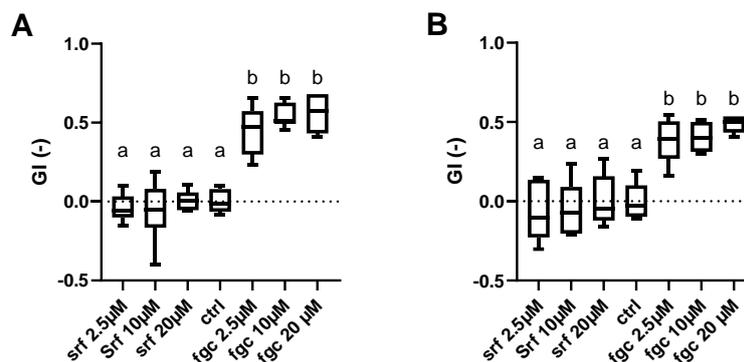
Figure 5 Growth inhibition factor of surfactin and fengycin treatments after 48 hours (A) and 96 hours (B). Boxes extend from 25th to 75th percentile and whiskers from min to max values. The central line is the median. Letters indicate significantly different groups (one-way ANOVA with Tukey's multiple comparison post-test).

Effect of srf and fgc on the spore germination of *B. cinerea*

An inhibitory effect of mycelial growth doesn't guarantee an impact of the same treatment on spore germination, and *vice versa*. To further characterize the direct antifungal properties of srf and fgc, their effect on spore germination was evaluated. Two protocols were considered, differing by the culture conditions. One was done entirely in microplates and the other used 15mL Falcon tubes for the cultures and microplates for absorbance measurements only. Absorbance measurements represent spore germination as it increases with the percentage of cells that germinate in the medium as well as with the length of the germ tubes. The first inhibition protocol was used for two independent experiments (Fig. 6A, B), with 3 repetitions for each. In the first replicate, the control showed, as expected, higher absorbance values than all other treatments throughout the experiment. However, after 36 hours, control values remained not significantly different than the 2.5µM srf and 2.5 µM and 20 µM fgc while a significant difference was observed with 10µM and 20µM srf and 10 µM fgc. Several values recorded were lower than the ones measured at the previous time point for the same wells, which is surprising as absorbance is expected to only increase relatively to the germination of spores. At the end of the experiment, white aggregates were noticed that had precipitated at the bottom of multiple wells (Annex 3). Precipitation of solutes could be an explanation of why measured absorbance decreased. Because of this phenomenon, no conclusions could be drawn of this first experiment. Agitation was thus increased for the second replicate of protocol N°1 (Fig. 6B). All treatments followed a similar sigmoid curve that didn't resemble the ones obtained in the first replicate. Although data dispersion is not similar for all treatments, there is no statistical differences between the treatments and the control (Fig. 7B). No effect of either CLP was observed on spore germination. However, white precipitates were also present at the end of the experiment (Annex 4), so no conclusion can be drawn from this replicate either. During the experiment following protocol N°2, no trend was noticeable before 48 hours (Fig. 6C). At this time, both the control and 2.5µM srf-treated cultures showed higher absorbance values. At the end of the experiment, those two treatments showed significantly higher values than the other treatments (Fig. 7C). A small inhibition of spore germination was thus observed for every treatment except 2.5µM srf in this experiment. However, white precipitates were noticed in the culture tubes as well as contamination in the media (Annex 5). Observation under microscope didn't allow identification of the components forming the white precipitates but they were also present in blanks (non-inoculated medium), which suggest that they are not spores nor mycelium. The main hypothesis is that all media were contaminated by another microorganism which composes the aggregates. Thus, none of the measured effects can be associated with the inhibition of spore germination with certitude. Some results seem to indicate a potential effect for concentrations above 2.5µM for both srf and fgc (Fig. 7A, C) but no effect was visible when repeating the first protocol (Fig. 7B). Some supplementary experiments are necessary to conclude on the effect of srf and fgc on spore germination of *B. cinerea*.
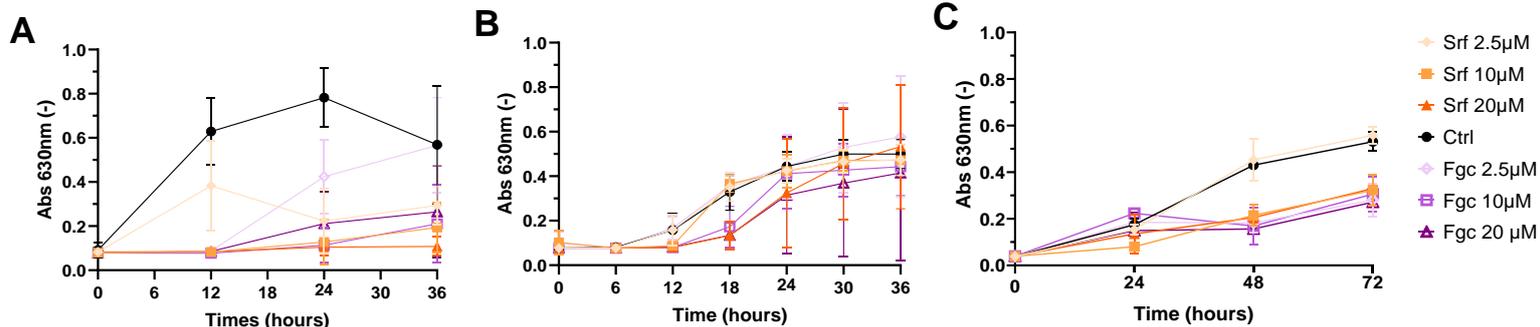
Figure 6 Measurement of surfactin and fengycin impact on B. cinerea *spore germination [A] Time-course evolution of* B. cinerea *spore germination in presence of either 2.5µM, 10µM or 20µM surfactin (srf) or 2.5µM, 10µM or 20µM fengycin (fgc) under protocol N°1, 1st repetition [B] Time-course evolution of* B. cinerea *spore germination in presence of either 2.5µM, 10µM or 20µM srf or 2.5µM, 10µM or 20µM fgc under protocol N°1, 2nd repetition [C] Time-course evolution of* B. cinerea *spore germination in presence of either 2.5µM, 10µM or 20µM srf or 2.5µM, 10µM or 20µM fgc under protocol N°2. Data are shown as mean ± SD, n=6 (from 2 independent triplicates).*
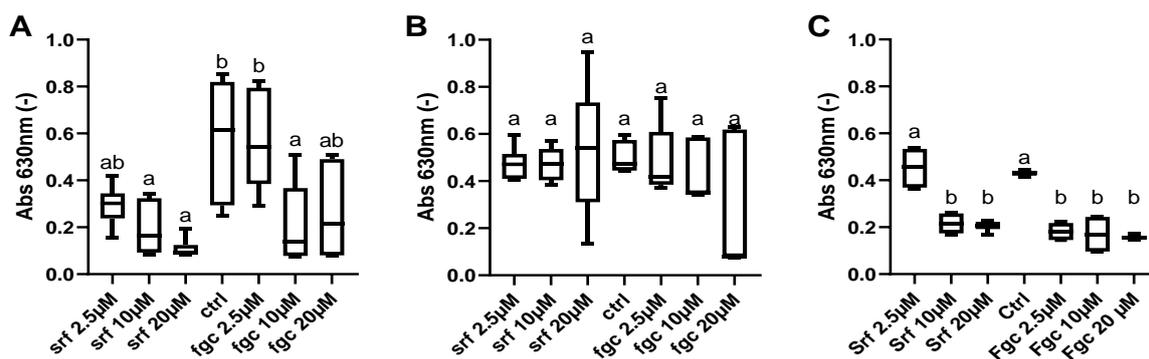
Figure 7 Absorbance values of surfactin (srf) and fengycin (fgc) treatments. [A] 1st repeat of protocol 1 after 36 hours [B] 2nd repeat of protocol 1 after 36 hours [C]Protocol 2 after 48 hours. Boxes extend from 25th to 75th percentile and whiskers from min to max values. The central line is the median. Letters indicate significantly different groups (one-way ANOVA with Tukey's multiple comparison post-test).

15

Early defense events induced by srf and fgc

After investigating the biocontrol potential of srf and fgc through direct interaction with pathogens, their indirect effect through elicitation of plant defense was studied. The stimulation of plant defense leads to multiple "early defense events" described in the introduction of this work. Here, the Ca^{2+} fluxes, ROS production and extracellular medium alkalinization have been examined as markers for *A. thaliana* immune stimulation. The $Ca^{2+}$ and ROS experiments have been conducted on fresh and 1-day-old protoplasts to evaluate the role of the cell wall in the plant response and medium alkalinization was assessed on whole roots to mimic natural conditions.

Calcium fluxes

The calcium fluxes were characterized by monitoring the cytosolic concentration of Ca^{2+} using two methods: Fluo-4 AM and aequorin, in order to compare each system response. Results obtained with the fluorescent probe Fluo-4 AM showed a constant augmentation of the fluorescence for all treatments (Fig. 8A, B). However, the slope of the curves differed for each treatment. Flagellin (flg) was similar to the control with fresh and 1-day-old protoplasts while both srf and chitin (cht) were significantly higher (Fig. 9A, B). In the case of fgc, different concentrations were tested. Although fgc curves at different concentrations were comprised between the control and 10 µM srf ones (Fig. 8C, D) no significant differences of calcium influx to the control were observed with fresh protoplasts (Fig. 9C). In the case of 1-day-old protoplasts, the calcium influx at fgc concentrations of 2.5µM and 10µM was significantly above the control but this was not the case for the 20µM concentration (Fig. 9D). Fluo-4 AM experiments revealed a similar increase in Ca^{2+} for srf and cht treatment in fresh and 1-day-old protoplasts. The fgc treatments had a small effect on fresh protoplasts after 6 minutes but no significant effect on 1-day-old protoplasts. No effect of the fgc concentration has been observed.

When aequorin was used to quantify $[Ca^{2+}]_{cyt}$ no differences were apparent between flg, srf and the control (Fig. 8E). Cht treatment presented a large peak from 1.5minutes to 6 minutes with fresh protoplasts but none with 1-day-old protoplasts (Fig. 8F). Cht treatment on fresh protoplasts is the only treatment that induced a observable influx of calcium with the aequorin method.

With aequorin, absolutely no effect can be seen except for cht on fresh protoplasts. As this corresponds to the highest signal in the Fluo-4 AM experiment, the absence of response with the aequorin method could be explained by its lower limit of detection compared to the Fluo-4 method.
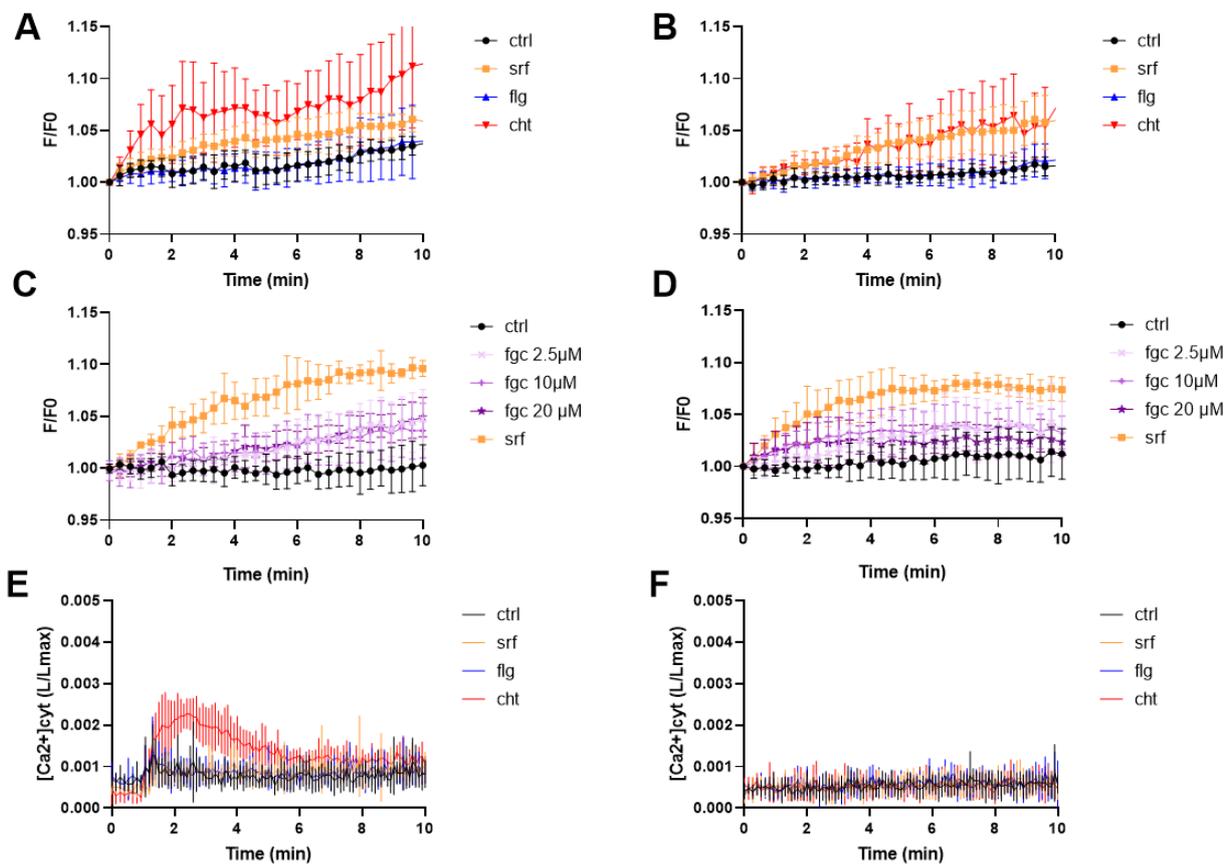
Figure 8 Measurement of calcium influx in root protoplasts [A, B] Change of $[Ca^{2+}]_{cyt}$ measured with fluo4-AM in Col-0 root protoplasts freshly isolated (A) or 1-day-old (B) following treatment with 10µM surfactin (srf), 1µM flagellin (flg) and 100µg/mL chitin (cht). [C, D] Change of $[Ca^{2+}]_{cyt}$ measured with fluo4-AM in Col-0 root protoplasts freshly isolated (C) or 1-day-old (D) following treatment with 10µM srf, and 2.5µM, 10µM and 20µM fengycin (fgc). [E, F] Change of $[Ca^{2+}]_{cyt}$ measured with aequorin in Col-0 root protoplasts freshly isolated (E) or 1-day-old (F) following treatment with 10µM srf, 1µM flg and 100µg/mL cht. Data are shown as mean ± SD, n=15 (from 5 independent triplicates) for A and B, n=9 (from 3 independent triplicates) for C and D, n=12 (from 6 independent duplicates) for E and n=8 (from 4 independent duplicates) for F.
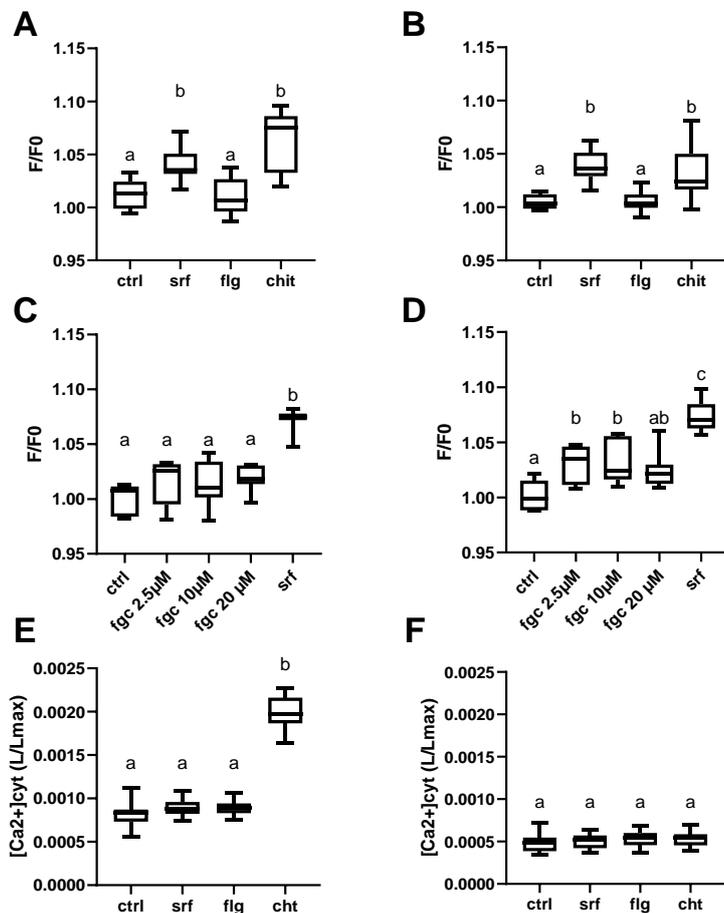
Figure 9 Concentration of cytosolic Ca^{2+} after treatments. [A, B] Fluorescence increase of Fluo-4 AM in fresh (A) and 1-day-old (B) protoplasts 5 minutes after treatment with surfactin (srf), flagellin (flg) and chitin (cht) [C, D] Fluorescence increase of Fluo-4 AM in fresh (C) and 1-day-old (D) protoplasts 5 minutes after treatment with srf at 10 µM and fengycin (fgc) at different concentrations [E, F] Integration of L/L_{MAX} values of aequorin between 1.5 and 4 minutes after treatment of fresh (E) and 1-day-old (F) protoplasts with srf, flg and cht. Boxes extend from 25th to 75th percentile and whiskers from min to max values. The central line is the median. Letters indicate significantly different groups (one-way ANOVA with Tukey's multiple comparison post-test).

17

Cytosolic ROS production

As established before, the production of intracellular ROS is one of the early defense events observed following surfactin treatment (Henry et al., 2011). Its production was measured using the fluorescence of the DCFH-DA probe. The fold increase is the ratio between the fluorescence increase for a given treatment and the control. Fresh protoplasts treated with flg and fgc followed a constant fluorescence increase similar to the control while srf and cht increased slightly faster (Fig. 10A, C). Thus, the fold increase of flg and fgc treatments, as the control, remained constant around 1 (Fig. 7E, G). With srf and cht, a large and small peak was visible in the first 20 minutes (Fig. 10E). However, because of the high standard deviations, only srf was statistically different from the control, not cht (Fig. 11A). The fluorescence measured on 1-day-old protoplasts was similar to the control after flg and fgc treatments (Fig. 10B) and their fold increase values stayed constant (Fig. 10F). Srf treatment led to a faster fluorescence increase that resulted in a non-significant small peak in fold increase values (Fig. 10B, F, 11B). After cht treatment, an even faster increase was noticed with a higher fold increase peak that was slightly delayed in comparison with srf and cht on fresh protoplasts (Fig. 10B, E, F). Unlike with fresh protoplasts only cht treatment was significantly different than others on 1-day-old protoplasts (Fig. 11B).

The flg and fgc treatments had no significant effect on ROS production in either fresh or 1-day-old protoplasts. However, on fresh protoplasts, intracellular ROS were produced under srf treatment and a smaller effect was noticeable with cht while on 1-day-old protoplasts, the effect of srf was less noticeable and cht was significantly different than all other treatments. This indicates that the presence of the cell wall possibly influences intracellular ROS accumulation under elicitation with cht and srf. Because the effect of the cell wall was different on the response of both treatments, the mechanisms through which they trigger ROS production may differ.
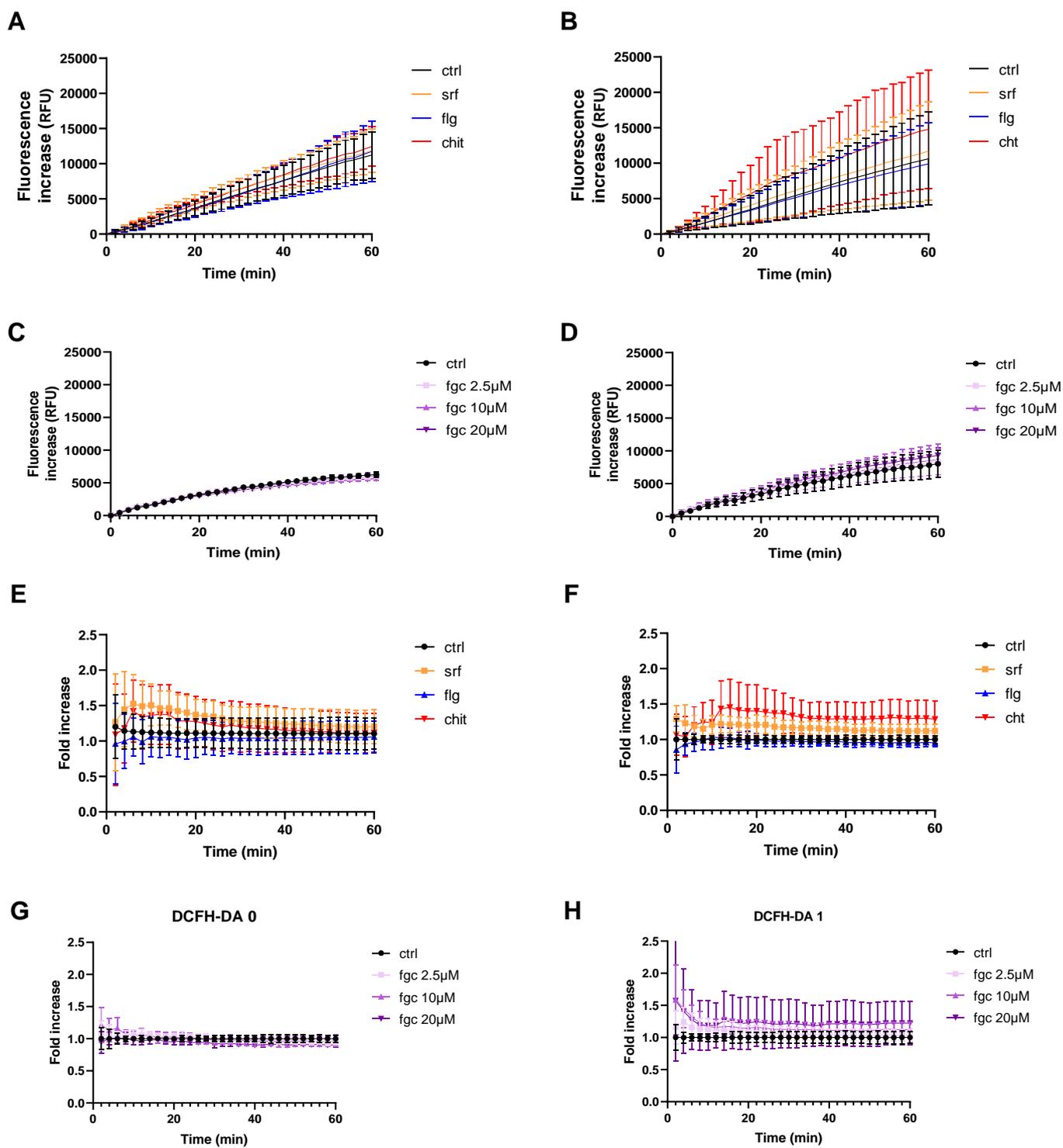
Figure 10 Measurement of cytosolic ROS production in root protoplasts. [A, B] Change of [ROS]$_{intra}$ measured with DCFH-DA in Col-0 root protoplasts freshly isolated (A) or 1-day-old (B) following treatment with 10µM surfactin (srf), 1µM flagellin (flg) and 100µg/mL chitin (cht). [C, D] Change of [ROS]$_{intra}$ measured with DCFH-DA in Col-0 root protoplasts freshly isolated (C) or 1-day-old (D) following treatment with 2.5µM, 10µM, 20µM fengycin (fgc) [E,F] Evolution of the fold increase measured with DCFH-DA in Col-0 root protoplasts freshly isolated (E) or 1-day-old (F) following treatment with 10µM srf, 1µM flg and 100µg/mL cht. [F] Evolution of the fold increase measured with DCFH-DA in Col-0 root protoplasts freshly isolated (G) or 1-day-old (H) following treatment with 2.5µM, 10µM, 20µM fgc. Data are shown as mean ± SD, n=14 (from 7 independent duplicates) for A, B, E and F, n=9 (from 3 independent triplicates) for C, D, G and H.
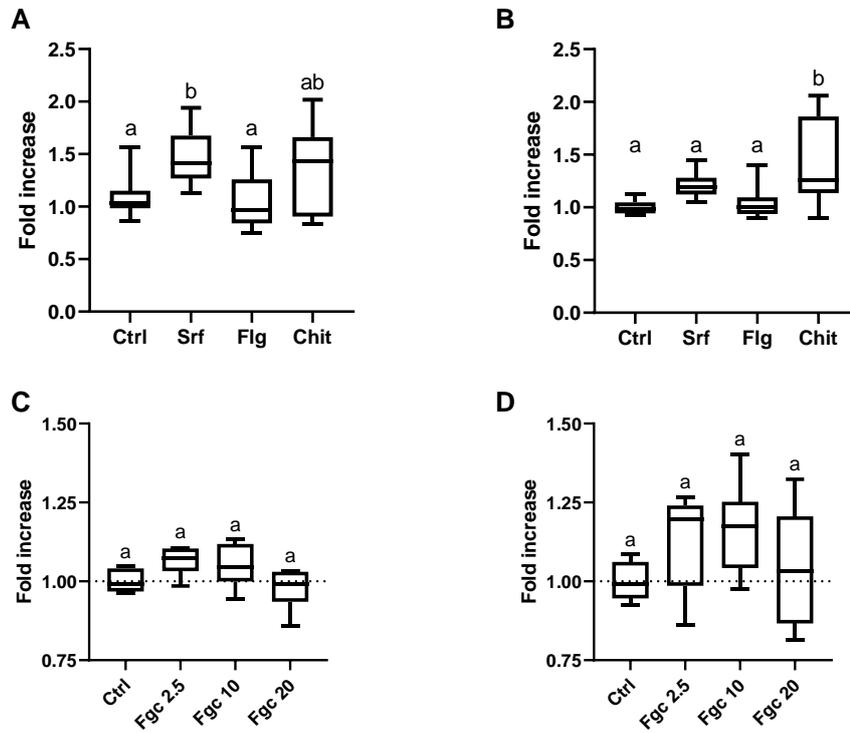
Figure 11 Fold increase values measured 14 minutes after treatments. [A, B] Surfactin (srf), flagellin (flg) and chitin (cht) treatments on fresh (A) and 1-day-old (B) protoplasts. [C, D] Fengycin (fgc) treatments at different concentrations on fresh (A) and 1-day-old (B) protoplasts. Boxes extend from 25th to 75th percentile and whiskers from min to max values. The central line is the median. Letters indicate significantly different groups (one-way ANOVA with Tukey's multiple comparison post-test).

Conductivity and pH variation around the roots

The third early defense event measured was the pH and conductivity changes in the extracellular root media. This event results from the ionic fluxes through the root cell membrane. After adding treatments to peripheral root medium, the pH (Fig. 12A) and conductivity (Fig. 12B) were directly recorded every 5 minutes. Triton X-100 (trt), which is a powerful detergent, was used as a positive treatment. It provoked cellular lysis, leading to higher solutes concentration in the medium, which resulted in a conductivity increase. The pH values of the control remained constant throughout the experiment. The pH of the srf-treated medium lowered from 5.45 to 5.22 after 40 minutes. Cht and trt treatment both made the medium more alkaline but the increase in pH was greater for trt (Fig. 12C). Concerning conductivity, it remained constant under control conditions (Fig 12B, D). Cht treatment increased conductivity steadily from 201μS/cm to 219μS/cm and srf from 211μS/cm to 239μS/cm during the 40 minutes recorded (Fig. 12D). Trt-treated medium rapidly increased from 220 to 270μS/cm in the first 10 minutes. The increase then slowed down and conductivity reached 285μS/cm at the last measurement. After 30 minutes, the trt treatment was significantly above others (Fig. 13D). Before drawing conclusions, the experiment should have been repeated more times. There was no noticeable effect of srf on pH while trt and cht provoked media alkalinization. The effect of cht treatment was smaller than trt. There may have been a slightly higher conductivity increase with cht and srf compared to the control, but data was not significant.
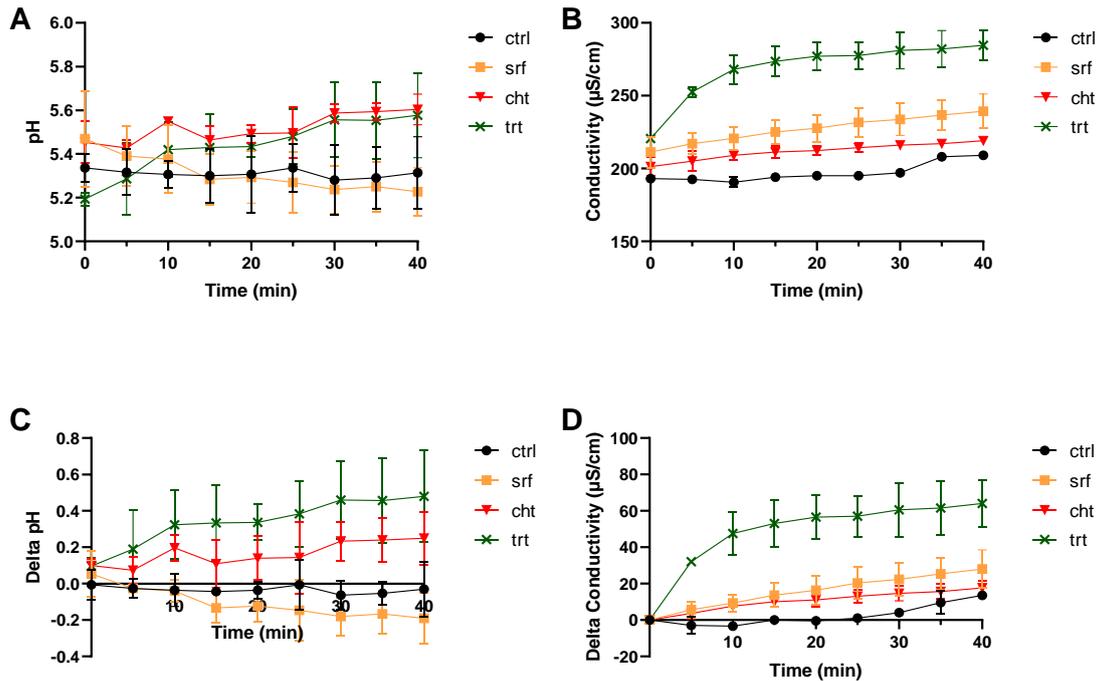
Figure 12 Variation of the extracellular root medium [A] Evolution of the pH of the extracellular root medium treated with 10µM surfactin (srf), 100µg/mL chitin (cht) and 0.9% triton X-100 (trt). [B] Evolution of the conductivity of the extracellular root medium treated with 10µM srf, 100µg/mL cht and 0.9% trt. [C] Evolution of the pH variation of the extracellular root medium treated with 10µM srf, 100µg/mL cht and 0.9% trt. [D] Evolution of the conductivity variation of the extracellular root medium treated with 10µM srf, 100µg/mL cht and 0.9% trt. Data are shown as mean ± SD, n=3 from 1 experiment.
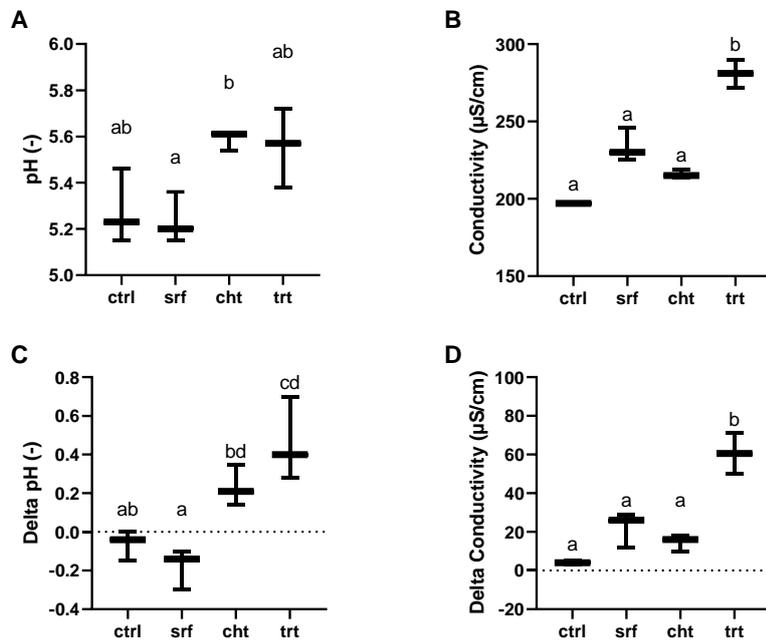
Figure 13 Variation of extracellular media 30 minutes after treatments with surfactin (srf), chitin (cht) and triton X-100 (trt) [A] pH values [B] Conductivity values [C] pH variation values [D] Conductivity variation values. Boxes extend from 25th to 75th percentile and whiskers from min to max values. The central line is the median. Letters indicate significantly different groups (one-way ANOVA with Tukey's multiple comparison post-test).

Effect of srf and fgc on membrane fluidity

After characterizing the potential direct and indirect effect of srf and fgc on *A. thaliana* protection , their putative molecular mechanism was investigated. As the main hypothesis for the plant protection by srf is the triggering of their immune defense via the interaction of srf with plant plasma membrane, the effect of srf on the membrane fluidity has been characterized and compared to the effect of flg and cht. In addition, the effect of different concentrations of fgc on membrane fluidity was also investigated, even though this lipopeptide is less susceptible to trigger the immune defense. For this purpose, two fluorescent probes have been used. The first is laurdan, which is a well-known probe for fluidity assessment. The second is di-4-ANEPPDHQ because it has been used in multiple studies on plant cells to probe plasma membrane organization (Gronnier et al., 2017; Sandor et al., 2016) and may react differently than laurdan (Amaro et al., 2017). Data was presented as the difference between GP calculated at each time point and GP measured before adding treatments. When measuring with laurdan, the flg and cht treatments gave similar curves to the control for both types of protoplasts (Fig. 14 A, B). These curves slowly increased of less than 0.1 unit during the 20 minutes experiment. The srf treatment resulted in significantly higher ΔGP values (Fig. 14A, B). Laurdan measurement of the membrane fluidity after fgc treatments seemed to follow the control for both fresh (Fig. 14C) and 1-day-old (Fig. 14D) protoplasts. Srf was used as a positive control in these experiments, its ΔGP values were above all other treatments. When measuring with di-4-ANEPPDHQ, flg and cht responses also gave similar curves to the control (Fig. 14E, F). With fresh protoplasts, they slowly increased of less than 0.05 units (Fig. 14E) and they remained relatively constant with 1-day-old protoplasts (Fig. 14F). The ΔGP values of the srf treatments were significantly above the others (Fig. 14E, F). Both probes gave similar results, indicating a rigidification of the plasma membrane in the presence of srf but no particular effect with the other treatments.
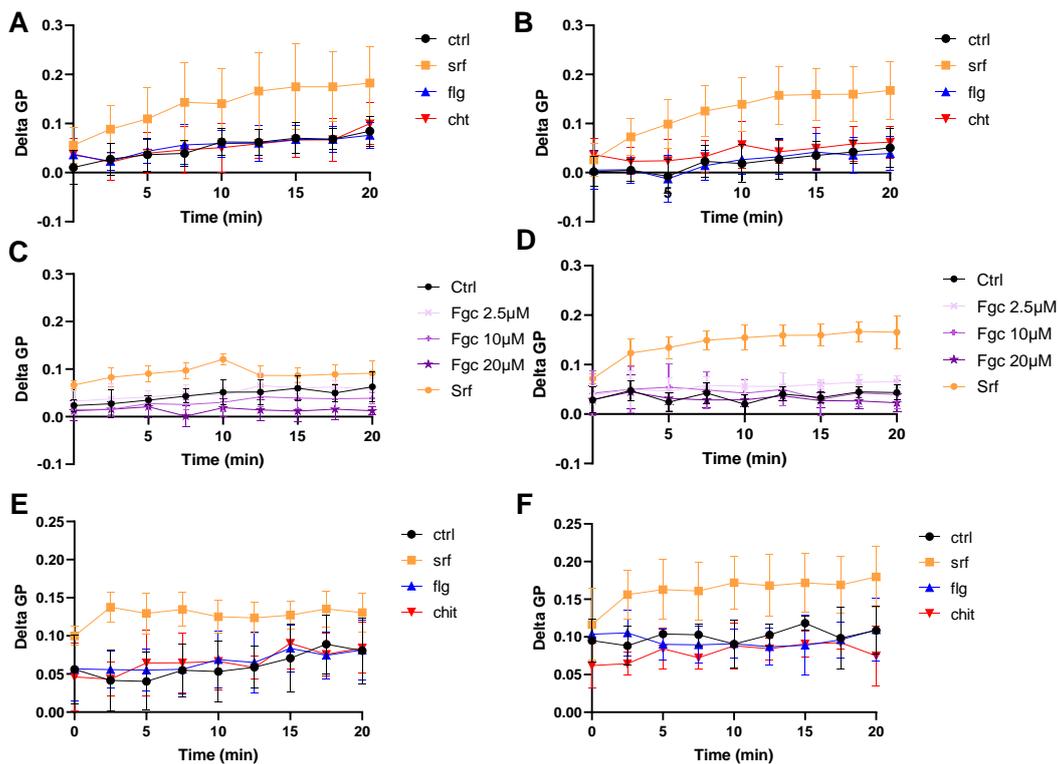
Figure 14 Measurement of plasma membrane fluidity in root protoplasts [A, B] Change of membrane fluidity measured with laurdan in Col-0 root protoplasts freshly isolated (A) or 1-day-old (B) following treatment with 10µM surfactin (srf), 1µM flagellin (flg) and 100µg/mL chitin (cht). [C, D] Change of membrane fluidity measured with laurdan in Col-0 root protoplasts freshly isolated (C) or 1-day-old (D) following treatment with 10µM srf and 2.5µM, 10µM and 20µM fengycin (fgc). [E, F] Change of membrane fluidity measured with di-4-ANNEPDHQ in Col-0 root protoplasts freshly isolated (E) or 1-day-old (F) following treatment with 10µM srf, 1µM flg and 100µg/mL cht. Error bars represent the SD of 6 duplicates for A, 8 duplicates for B, 4 duplicates for C and 3 duplicates for D. Data are shown as mean ± SD, n=12 (from 6 independent duplicates) for A, n=16 (from 8 independent duplicates) for B, n=6 (from 3 independent duplicates) for C, D and F, n=8 (from 4 independent duplicates) for E.
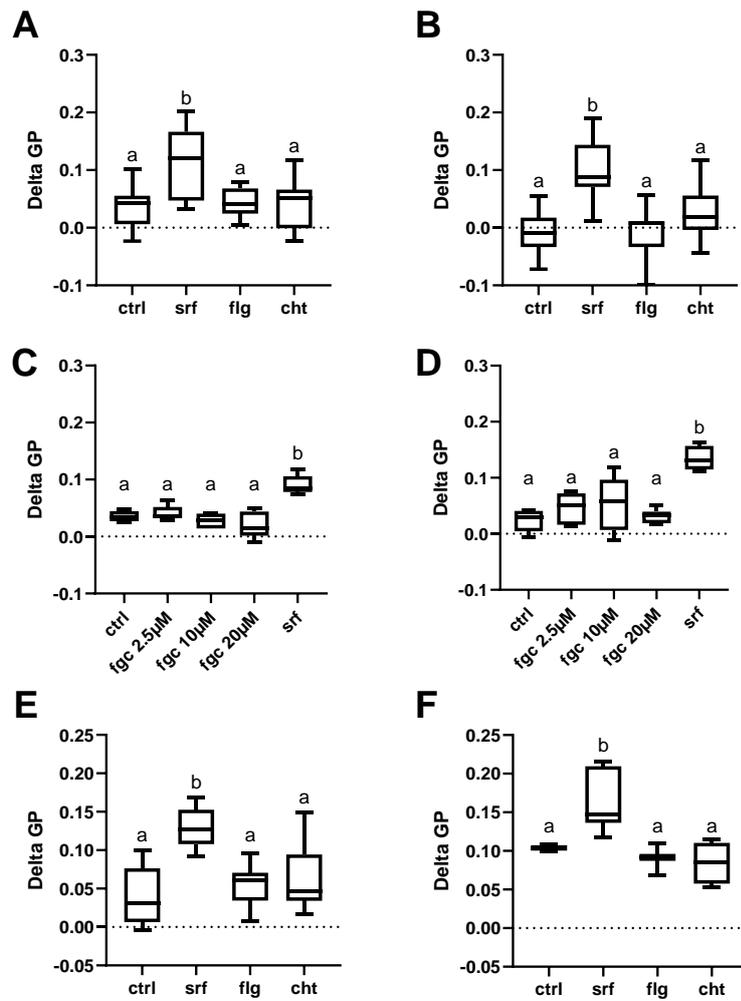
Figure 15 ΔGP values 5 minutes after treatments. [A, B] Laurdan measurements on fresh (A) and 1-day-old (B) protoplasts treated with surfactin (srf), flagellin (flg) and chitin (cht) [C, D] Laurdan measurements on fresh (C) and 1-day-old (D) protoplasts treated with srf and fengycin (fgc) [E, F] Di-4-ANNEPDHQ measurements on fresh (E) and 1-day-old (F) protoplasts treated with srf, flg and cht. Boxes extend from 25th to 75th percentile and whiskers from min to max values. The central line is the median. Letters indicate significantly different groups (one-way ANOVA with Tukey's multiple comparison post-test).

Discussion

Among *Bacillus* metabolites of interest, surfactin (srf) has been widely studied for its plant protection activity. As mentioned in the introduction, its direct effect on various pathogens has been analyzed by different research groups. While its antiviral activity against enveloped virus is proved (Kracht et al., 1999), its antifungal and antibacterial properties are controversial. To assess its inhibition potential against fungal pathogens, mycelial growth rate and spore germination experiment were conducted on *B. cinerea*, a model fungus. No effect of srf at concentrations up to 20μM has been observed on the mycelial growth of *B. cinerea*. These results align with a recent study that also did not measure a significant effect for the same range of concentrations (Xiao et al., 2023). They nevertheless observed inhibition with higher concentrations of srf. It is important to note that their results are only based on one triplicate and that the formula they used for the inhibition rate of mycelial growth amplifies their calculated values. The effect of srf at higher concentrations should thus be confirmed. Another article claiming that srf has antifungal properties is (G A et al., 2013). However, the concentration they used is not specified and the effect could result from other molecules than srf present in the treatments. Concerning fengycin (fgc), its already studied inhibitory effect on mycelial growth (Tao et al., 2011; Vanittanakom et al., 1986) has been confirmed in our study. In the literature, some works report a small dose effect of fgc on mycelial growth (Tao et al., 2011), which could explain why no differences were observed between the relatively close concentrations tested in our study. Other works report an all-or-none effect of fgc, where permeabilization of fungi membrane either results in complete leakage of the cell content or does not happen at all (Patel et al., 2011). As membrane permeabilization is the supposed mechanism of fgc antifungal property (Patel et al., 2011; Vanittanakom et al., 1986), this effect can be the cause of an all-or-none effect of fgc on mycelial growth as observed by (Wise et al., 2014), which corresponds to what we observed.

The effect of both srf and fgc on spore germination of *B. cinerea* cannot be asserted with the results of our experiments. According to literature, a concentration-dependent effect of fgc on spore germination of fungal pathogens has already been reported (Tao et al., 2011). Concerning srf, the same recent study as above (Xiao et al., 2023) reported a small, dose-dependent effect on spore germination. However, srf concentrations up to 20μM had a low inhibition effect on the triplicate they tested. In order to further investigate the activity of srf on spore germination, protocols should be revised. The first protocol, where spores were cultured in microplates, could display better results by improving the sterile conditions of the experiment. However, the second protocol, with spore suspension in 15mL Falcon tubes, is more promising. Although more time consuming, the second method allows greater agitation and counting of germinated spores under microscope. This avoids errors in absorbance measurements that depend on both the percentage of germination and the length of the germ tube of spores. Suggested improvements are thus to repeat the second protocol with adjustments to avoid contamination and to focus on germination percentage rather than absorbance values.

Concerning the indirect biocontrol effect of the CLPs through plant stimulation, different early immune events including calcium influx, ROS production, extracellular medium alkalinization and conductivity were measured. Srf and chitin (cht) both produced calcium influx measured with the Fluo-4 AM probe but only cht on fresh protoplasts had a measurable effect with the aequorin method. This could be explained by a lower limit of detection of the aequorin method, as cht on fresh protoplasts was the highest response in Fluo-4 AM experiments. Previous experiments from our laboratory have already shown a calcium influx following srf treatment when measured with aequorin (Pršić et al., 2023). The graph obtained was similar to cht results from this study. Because the experimental set up was the same as ours, the hypothesis could be made that the previous results presented a higher response in calcium concentration than in this study, being thus detectable with the aequorin system. It is also interesting to note that, during the previous experiment, protoplasts also presented a response after flagellin (flg) treatments (Pršić et al., 2023). In

this study, flg followed the control in every experiment. It would be interesting to verify if the flg extract used has not been degraded in the meantime. Fgc dose experiments revealed a calcium influx slightly higher than control but not significant for each concentration on fresh protoplasts and significant but weak on 1-day-old protoplasts. As for the antifungal experiments, similarity of the response regardless of concentration can be explained either by a small dose effect and relatively similar concentrations tested in our study or by an all-or-none response. Lower repetition number for the fgc tests could also affect the reliability of the results. The low intensity of the calcium influx after fgc treatments could relate to the low ISR effect recorded for this CLP (Ongena et al., 2007).

Intracellular ROS production followed similar trends. Fgc treatments resulted in ROS production slightly higher than control but not significant for all the concentrations tested. Concerning srf and cht, they showed a similar response but srf treatment led to higher ROS production in fresh protoplasts while it was cht in 1-day-old protoplasts. As observed in cell suspension of tobacco roots (Henry et al., 2011), the intracellular burst was rapid on fresh protoplasts. However, it was more delayed on 1-day-old cells, especially after cht treatment. The change in timing and intensity of the response on both ages of protoplasts reinforces the hypothesis that the cell wall influences ROS production (Ledoux et al., 2014). ROS production depends on various sources that are still under study (Torres, 2010). Peroxidases from the cell wall are reported to amplify the production (Torres, 2010) which could explain the delayed peak observed for cht treatments on 1-day-old protoplasts. As this delay is not observed after srf treatment, it could be an effect specific to PTI response, supporting the evidence that srf triggers different mechanisms.

The alkalinization and conductivity of extracellular root media had previously been reported for srf treatment on tobacco root cell suspension (Jourdan et al., 2009). In our study, srf did not seem to disrupt the membrane but the expected alkalinization could not be measured. On the contrary, a slight, non-significant acidification of the medium could be noticed. This result is also contradictory with previous results obtained by our research group on the same system (Pršić et al., 2023). One explanation could be an error due to treatment preparation, as the three repetitions of the experiment were done using the same treatment solutions. Another explanation would be the impact of biological variation, as two different *A. thaliana* plantlets do not respond in the same exact way to the same treatment. However, the error does not come from the design of the experiment as treatment with triton X-100 (trt), a powerful detergent that disrupts the plasma membrane, provoked the highest alkalinization with the greatest increase in conductivity. For cht, a small alkalinization was measured, in accordance with PTI responses (Baureithel et al., 1994) but nearly no increase in conductivity was measured, indicating that it did not disrupt the plasma membrane. As the experiment was only conducted once in triplicates, repetition should be done to confirm the results obtained.

When focusing on the first two early events measured, srf, that elicits ISR, presented similar responses to cht, an elicitor of PTI. However, the differences observed in intracellular ROS production on 1-day-old protoplasts supports that distinct mechanisms lead to this signaling, with a contribution of the cell wall. As discussed above, flg produced similar responses to srf in previous experiments (Pršić et al., 2023). However, it may have been denatured in the meantime and thus be ineffective in these tests. Fgc triggered only small calcium fluxes and no ROS production, which correspond to the small ISR effect associated with it (Ongena et al., 2007).

It is known that srf interacts with membrane lipids (Gilliard et al., 2022). To further investigate the hypothesis that the primary steps of the defense response are related to a physical change of the plant plasma membrane (Henry et al., 2011; Pršić & Ongena, 2020), fluidity measurements of the plasma membrane were conducted on root protoplasts. Throughout all experiments and whatever the fluorescent probe used (laurdan or di-4-ANEPPDHQ), only srf treatments differed from the control and increased plasma membrane rigidity, in accordance with previous results from our research group (Pršić

et al., 2023). Rigidification of the membrane changes its properties such as tension. Mechanosensitive (MS) ion channels are a type of channels of the plasma membrane that are activated by changes in membrane tension (Yoshimura et al., 2021). The interaction of srf with the plant plasma membrane causes changes in rigidity that could activate those MS channels, instigating ion fluxes, that would then lead to the defense response. Cht perception by the cell is realized via its interaction with PRRs at the cell surface (Boller & Felix, 2009). The signal is then transmitted inside the cells via transmembrane proteins (Dievart et al., 2020). The absence of direct interaction of cht with the membrane is thus not surprising. Some studies have reported a short transitory modification of membrane fluidity after MAMP perception (Sandor et al., 2016). However, this effect is due to reorganization of the membrane during PTI response (Sandor et al., 2016) and is not similar to the one induced by srf.

Conclusion

Our experiments confirm that both CLPs, srf and fgc, present interesting biocontrol effects. However, the mechanisms through which they induced plant protection differ. Fgc has an inhibitory effect on *B. cinerea* likely due to its permeabilizing activity on the fungal membrane. On contrary, srf does not present such direct effect against *B. cinerea.*

Srf triggers multiple events related to the early defense of plants. These effects have not been observed after fcg treatments at the tested concentrations. The differences observed between the responses induced after srf and cht treatments gives evidence that both molecules activate the defense signaling through distinct mechanisms. Membrane fluidity assessment confirms that srf induces a rigidification of the plant plasma membrane of *A. thaliana* root protoplasts. These results support the hypothesis that the interaction of srf with the lipids of the plasma membrane could initiate the ISR response through activation of mechanosensitive (MS) ion channels in the membrane. To further study this hypothesis, identification of the MS channels involved as well as characterization of the reactions they trigger should be looked at.

While the implication of CLPs produced by bacteria of the *Bacillus* genus in biocontrol activity is undeniable, their diverse action mechanisms make them synergistic. When developing alternatives to chemical pesticides, this aspect should thus be kept in mind. Using a combination of srf and fgc in field applications would exploit both the direct and indirect biocontrol properties, improving the efficiency of treatments. Exploring the combined use of other *Bacillus* metabolites would then be interesting in order to further develop this efficiency.

Student contribution

The student searched the literature in order to improve his knowledge on the subject of the study. He synthesized the general information necessary to understand this study in an introduction and described in detail the strategy behind the experimentation. He put together protocols for the experiments in the phytopathology laboratory after comparing multiple research papers and conducted them. The student also modified the protocols that did not provide satisfactory results by using his understanding of the experiments and ran supplementary tests to better understand the acquired data. The planning abilities of the student allowed him to realize the multiple repetition of the experiments planned in the time available. He realized multiple tests requiring different skills and contributed to the common work of the laboratory that welcomed him during this project. He treated the data he obtained, built various graphics and organized his results for interpretation in this work. The student organized the data for storage in the archives of the laboratory. He learned to use new programs (Prism, ImageJ) to help him in his work. He performed statistical analysis of the data and reported them here. The student interpreted the results and compared them to the literature, using critical thinking and providing hypothesis to support his claims. Finally, he contextualized the interpretation of his results and redacted this study to present them.

Bibliography

Amaro, M., Reina, F., Hof, M., Eggeling, C., & Sezgin, E. (2017). Laurdan and Di-4-ANEPPDHQ probe different properties of the membrane. *Journal of Physics D: Applied Physics*, *50*(13), 134004. https://doi.org/10.1088/1361-6463/aa5dbc

Arima, K., Kakinuma, A., & Tamura, G. (1968). Surfactin, a crystalline peptidelipid surfactant produced by Bacillussubtilis : Isolation, characterization and its inhibition of fibrin clot formation. *Biochemical and Biophysical Research Communications*, *31*(3), 488-494. https://doi.org/10.1016/0006-291X(68)90503-2

Bais, H. P., Fall, R., & Vivanco, J. M. (2004). Biocontrol of Bacillus subtilis against Infection of Arabidopsis Roots by Pseudomonas syringae Is Facilitated by Biofilm Formation and Surfactin Production. *Plant Physiology*, *134*(1), 307-319. Scopus. https://doi.org/10.1104/pp.103.028712

Boller, T., & Felix, G. (2009). A Renaissance of Elicitors : Perception of Microbe-Associated Molecular Patterns and Danger Signals by Pattern-Recognition Receptors. *Annual Review of Plant Biology*, *60*(1), 379-406. https://doi.org/10.1146/annurev.arplant.57.032905.105346

Bonmatin, J.-M., Laprevote, O., & Peypoux, F. (2003). Diversity Among Microbial Cyclic Lipopeptides : Iturins and Surfactins. Activity-Structure Relationships to Design New Bioactive Agents. *Combinatorial Chemistry & High Throughput Screening*, *6*(6), 541-556. https://doi.org/10.2174/138620703106298716

Cao, Y., Liang, Y., Tanaka, K., Nguyen, C. T., Jedrzejczak, R. P., Joachimiak, A., & Stacey, G. (2014). The kinase LYK5 is a major chitin receptor in Arabidopsis and forms a chitin-induced complex with related kinase CERK1. *ELife*, *3*, e03766. https://doi.org/10.7554/eLife.03766

Caulier, S., Gillis, A., Colau, G., Licciardi, F., Liépin, M., Desoignies, N., Modrie, P., Legrève, A., Mahillon, J., & Bragard, C. (2018). Versatile Antagonistic Activities of Soil-Borne Bacillus spp. And Pseudomonas spp. Against Phytophthora infestans and Other Potato Pathogens. *Frontiers in Microbiology*, *9*. https://www.frontiersin.org/articles/10.3389/fmicb.2018.00143

Chen, Y., Yan, F., Chai, Y., Liu, H., Kolter, R., Losick, R., & Guo, J. (2013). Biocontrol of tomato wilt disease by Bacillus subtilis isolates from natural environments depends on conserved genes mediating biofilm formation. *Environmental Microbiology*, *15*(3), 848-864. https://doi.org/10.1111/j.1462-2920.2012.02860.x

Chinchilla, D., Zipfel, C., Robatzek, S., Kemmerling, B., Nürnberger, T., Jones, J. D. G., Felix, G., & Boller, T. (2007). A flagellin-induced complex of the receptor FLS2 and BAK1 initiates plant defence. *Nature*, *448*(7152), 497-500. https://doi.org/10.1038/nature05999

Clerck, C. D., Maso, S. D., Parisi, O., Dresen, F., Zhiri, A., & Jijakli, M. H. (2020). Screening of Antifungal and Antibacterial Activity of 90 Commercial Essential Oils against 10 Pathogens of Agronomical Importance. *Foods (Basel, Switzerland)*, *9*(10), 1418. https://doi.org/10.3390/foods9101418

Cocco, P. (2016). Pesticides and Human Health. In P. Cocco, *Oxford Research Encyclopedia of Environmental Science*. Oxford University Press. https://doi.org/10.1093/acrefore/9780199389414.013.82

Dean, R., Van Kan, J. A. L., Pretorius, Z. A., Hammond-Kosack, K. E., Di Pietro, A., Spanu, P. D., Rudd, J. J., Dickman, M., Kahmann, R., Ellis, J., & Foster, G. D. (2012). The Top 10 fungal pathogens in molecular plant pathology : Top 10 fungal pathogens. *Molecular Plant Pathology*, *13*(4), 414-430. https://doi.org/10.1111/j.1364-3703.2011.00783.x

DeFalco, T. A., & Zipfel, C. (2021). Molecular mechanisms of early plant pattern-triggered immune signaling. *Molecular Cell*, *81*(17), 3449-3467. https://doi.org/10.1016/j.molcel.2021.07.029

Falhof, J., Pedersen, J. T., Fuglsang, A. T., & Palmgren, M. (2016). Plasma Membrane H+-ATPase Regulation in the Center of Plant Physiology. *Molecular Plant*, *9*(3), 323-337. https://doi.org/10.1016/j.molp.2015.11.002

Faretra, F., & Pollastro, S. (1991). Genetic basis of resistance to benzimidazole and dicarboximide fungicides in Botryotinia fuckeliana (Botrytis cinerea). *Mycological Research*, *95*(8), 943-951. https://doi.org/10.1016/S0953-7562(09)80091-9

Fira, D., Dimkić, I., Berić, T., Lozo, J., & Stanković, S. (2018). Biological control of plant pathogens by Bacillus species. *Journal of Biotechnology*, *285*, 44-55. https://doi.org/10.1016/j.jbiotec.2018.07.044

Furt, F., Simon-Plas, F., & Mongrand, S. (2011). Lipids of the Plant Plasma Membrane. In A. S. Murphy, B. Schulz, & W. Peer (Éds.), *The Plant Plasma Membrane* (p. 3-30). Springer. https://doi.org/10.1007/978-3-642-13431-9_1

G A, P., A, T., E, K. l, & R, S. (2013). Antifungal and antibacterial properties of surfactin isolated from Bacillus subtilis growing on molasses. *African Journal of Microbiology Research*, *7*(25), 3165-3170. https://doi.org/10.5897/AJMR2013.5565

Galli, G., Rodriguez, F., Cosmina, P., Pratesi, C., Nogarotto, R., & de Ferra; Guido Grandi, F. (1994). Characterization of the surfactin synthetase multi-enzyme complex. *Biochimica et Biophysica Acta (BBA) - Protein Structure and Molecular Enzymology*, *1205*(1), 19-28. https://doi.org/10.1016/0167-4838(94)90087-6

Gerber, I. B., Zeidler, D., Durner, J., & Dubery, I. A. (2004). Early perception responses of Nicotiana tabacum cells in response to lipopolysaccharides from Burkholderia cepacia. *Planta*, *218*(4), 647-657. https://doi.org/10.1007/s00425-003-1142-0

Gilliard, G., Furlan, A. L., Smeralda, W., Pršić, J., & Deleu, M. (2022). Added Value of Biophysics to Study Lipid-Driven Biological Processes : The Case of Surfactins, a Class of Natural Amphiphile Molecules. *International Journal of Molecular Sciences*, *23*(22), Article 22. https://doi.org/10.3390/ijms232213831

Gilliard, G., Huby, E., Cordelier, S., Ongena, M., Dhondt-Cordelier, S., & Deleu, M. (2021). Protoplast : A Valuable Toolbox to Investigate Plant Stress Perception and Response. *Frontiers in Plant Science*, *12*. https://www.frontiersin.org/articles/10.3389/fpls.2021.749581

Gómez-Gómez, L., & Boller, T. (2000). FLS2. *Molecular Cell*, *5*(6), 1003-1011. https://doi.org/10.1016/S1097-2765(00)80265-8

Goñi, F. M. (2019). "Rafts" : A nickname for putative transient nanodomains. *Chemistry and Physics of Lipids*, *218*, 34-39. https://doi.org/10.1016/j.chemphyslip.2018.11.006

Gronnier, J., Crowet, J.-M., Habenstein, B., Nasir, M. N., Bayle, V., Hosy, E., Platre, M. P., Gouguet, P., Raffaele, S., Martinez, D., Grelard, A., Loquet, A., Simon-Plas, F., Gerbeau-Pissot, P., Der, C., Bayer, E. M., Jaillais, Y., Deleu, M., Germain, V., … Mongrand, S. (2017). Structural basis for plant plasma membrane protein dynamics and organization into functional nanodomains. *eLife*, *6*, e26404. https://doi.org/10.7554/eLife.26404

Hajam, I. A., Dar, P. A., Shahnawaz, I., Jaume, J. C., & Lee, J. H. (2017). Bacterial flagellin—A potent immunomodulatory agent. *Experimental & Molecular Medicine*, *49*(9), e373-e373. https://doi.org/10.1038/emm.2017.172

Henry, G., Deleu, M., Jourdan, E., Thonart, P., & Ongena, M. (2011). The bacterial lipopeptide surfactin targets the lipid fraction of the plant plasma membrane to trigger immune-related defence responses. *Cellular Microbiology*, *13*(11), 1824-1837. https://doi.org/10.1111/j.1462-5822.2011.01664.x

Janeway, C. A., & Medzhitov, R. (2002). Innate Immune Recognition. *Annual Review of Immunology*, *20*(1), 197-216. https://doi.org/10.1146/annurev.immunol.20.083001.084359

Jourdan, E., Henry, G., Duby, F., Dommes, J., Barthélemy, J. P., Thonart, P., & Ongena, M. (2009). Insights into the defense-related events occurring in plant cells following perception of surfactin-type lipopeptide from Bacillus subtilis. *Molecular Plant-Microbe Interactions: MPMI*, *22*(4), 456-468. https://doi.org/10.1094/MPMI-22-4-0456

Kakinuma, A., Ouchida, A., Shima, T., Sugino, H., Isono, M., Tamura, G., & Arima, K. (1969). Confirmation of the Structure of Surfactin by Mass Spectrometry. *Agricultural and Biological Chemistry*, *33*(11), 1669-1671. https://doi.org/10.1080/00021369.1969.10859524

Kakinuma, A., Sugino, H., Isono, M., Tamura, G., & Arima, K. (1969). Determination of Fatty Acid in Surfactin and Elucidation of the Total Structure of Surfactin. *Agricultural and Biological Chemistry*, *33*(6), 973-976. https://doi.org/10.1080/00021369.1969.10859409

Kamilova, F., Validov, S., Azarova, T., Mulders, I., & Lugtenberg, B. (2005). Enrichment for enhanced competitive plant root tip colonizers selects for a new class of biocontrol bacteria. *Environmental Microbiology*, *7*(11), 1809-1817. https://doi.org/10.1111/j.1462-2920.2005.00889.x

Kanchiswamy, C. N., Malnoy, M., Occhipinti, A., & Maffei, M. E. (2014). Calcium Imaging Perspectives in Plants. *International Journal of Molecular Sciences*, *15*(3), Article 3. https://doi.org/10.3390/ijms15033842

Kinsinger, R. F., Shirk, M. C., & Fall, R. (2003). Rapid surface motility in Bacillus subtilis is dependent on extracellular surfactin and potassium ion. *Journal of Bacteriology*, *185*(18), 5627-5631. Scopus. https://doi.org/10.1128/JB.185.18.5627-5631.2003

Koornneef, M., & Meinke, D. (2010). The development of Arabidopsis as a model plant. *The Plant Journal*, *61*(6), 909-921. https://doi.org/10.1111/j.1365-313X.2009.04086.x

Köster, P., DeFalco, T. A., & Zipfel, C. (2022). Ca2+ signals in plant immunity. *The EMBO Journal*, *41*(12), e110741. https://doi.org/10.15252/embj.2022110741

Kracht, M., Rokos, H., Özel, M., Kowall, M., Pauli, G., & Vater, J. (1999). Antiviral and Hemolytic Activities of Surfactin Isoforms and Their Methyl Ester Derivatives. *The Journal of Antibiotics*, *52*(7), 613-619. https://doi.org/10.7164/antibiotics.52.613

Krishnan, N., Velramar, B., & Velu, R. K. (2019). Investigation of antifungal activity of surfactin against

mycotoxigenic phytopathogenic fungus Fusarium moniliforme and its impact in seed germination and

mycotoxicosis. *Pesticide Biochemistry and Physiology*, *155*, 101-107.

https://doi.org/10.1016/j.pestbp.2019.01.010

Kumar, J., Ramlal, A., Mallick, D., & Mishra, V. (2021). An Overview of Some Biopesticides and Their Importance in

Plant Protection for Commercial Acceptance. *Plants*, *10*(6), 1185. https://doi.org/10.3390/plants10061185

Leclère, V., Marti, R., Béchet, M., Fickers, P., & Jacques, P. (2006). The lipopeptides mycosubtilin and surfactin

enhance spreading of Bacillus subtilis strains by their surface-active properties. *Archives of Microbiology*,

186(6), 475-483. Scopus. https://doi.org/10.1007/s00203-006-0163-z

Lertcanawanichakul, M., & Sawangnop, S. (2008). A Comparison of Two Methods Used for Measuring the

Antagonistic Activity of Bacillus Species. *Walailak Journal of Science and Technology (WJST)*, *5*(2), Article 2.

Lilge, L., Ersig, N., Hubel, P., Aschern, M., Pillai, E., Klausmann, P., Pfannstiel, J., Henkel, M., Heravi, K. M., &

Hausmann, R. (2022). Surfactin Shows Relatively Low Antimicrobial Activity against Bacillus subtilis and

Other Bacterial Model Organisms in the Absence of Synergistic Metabolites. *Microorganisms*, *10*.

https://doi.org/10.3390/microorganisms10040779

Matzinger, P. (2002). The Danger Model : A Renewed Sense of Self. *Science*, *296*(5566), 301-305.

https://doi.org/10.1126/science.1071059

Meena, K. R., Sharma, A., Kumar, R., & Kanwar, S. S. (2020). Two factor at a time approach by response surface

methodology to aggrandize the Bacillus subtilis KLP2015 surfactin lipopeptide to use as antifungal agent.

Journal of King Saud University - Science, *32*(1), 337-348. https://doi.org/10.1016/j.jksus.2018.05.025

Merzendorfer, H. (2011). The cellular basis of chitin synthesis in fungi and insects : Common principles and

differences. *European Journal of Cell Biology*, *90*(9), 759-769. https://doi.org/10.1016/j.ejcb.2011.04.014

Ongena, M., & Jacques, P. (2008). Bacillus lipopeptides : Versatile weapons for plant disease biocontrol. *Trends in

Microbiology*, *16*(3), 115-125. https://doi.org/10.1016/j.tim.2007.12.009

Ongena, M., Jacques, P., Touré, Y., Destain, J., Jabrane, A., & Thonart, P. (2005). Involvement of fengycin-type

lipopeptides in the multifaceted biocontrol potential of Bacillus subtilis. *Applied Microbiology and

Biotechnology*, *69*(1), 29-38. https://doi.org/10.1007/s00253-005-1940-3

Ongena, M., Jourdan, E., Adam, A., Paquot, M., Brans, A., Joris, B., Arpigny, J.-L., & Thonart, P. (2007). Surfactin and fengycin lipopeptides of Bacillus subtilis as elicitors of induced systemic resistance in plants. *Environmental Microbiology*, *9*(4), 1084-1090. https://doi.org/10.1111/j.1462-2920.2006.01202.x

Pandin, C., Le Coq, D., Canette, A., Aymerich, S., & Briandet, R. (2017). Should the biofilm mode of life be taken into consideration for microbial biocontrol agents? *Microbial Biotechnology*, *10*(4), 719-734. https://doi.org/10.1111/1751-7915.12693

Peypoux, F., Bonmatin, J. M., & Wallach, J. (1999). Recent trends in the biochemistry of surfactin. *Applied Microbiology and Biotechnology*, *51*(5), 553-563. Scopus. https://doi.org/10.1007/s002530051432

Popp, J., Pető, K., & Nagy, J. (2013). Pesticide productivity and food security. A review. *Agronomy for Sustainable Development*, *33*(1), 243-255. https://doi.org/10.1007/s13593-012-0105-x

Pršić, J., Gilliard, G., Ibrahim, H., Argüelles-Arias, A., Rondelli, V., Crowet, J.-M., Genva, M., Luzuriaga-Loaiza, W. P., Deboever, E., Nasir, M. N., Lins, L., Mathelie-Guinlet, M., Boubsi, F., Eschrig, S., Ranf, S., Dorey, S., Coninck, B. D., Nürnberger, T., Mongrand, S., … Ongena, M. (2023). *Mechanosensing and Sphingolipid-Docking Mediate Lipopeptide-Induced Immunity in* Arabidopsis [Preprint]. Plant Biology. https://doi.org/10.1101/2023.07.04.547613

Pršić, J., & Ongena, M. (2020). Elicitors of Plant Immunity Triggered by Beneficial Bacteria. *Frontiers in Plant Science*, *11*. https://www.frontiersin.org/articles/10.3389/fpls.2020.594530

Pruitt, R. E., Bowman, J. L., & Grossniklaus, U. (2003). Plant genetics : A decade of integration. *Nature Genetics*, *33*(S3), 294-304. https://doi.org/10.1038/ng1108

Qiu, L., Wang, Y., & Qu, H. (2020). Loading calcium fluorescent probes into protoplasts to detect calcium in the flesh tissue cells of Malus domestica. *Horticulture Research*, *7*(1), Article 1. https://doi.org/10.1038/s41438-020-0315-3

Ramey, B. E., Koutsoudis, M., Bodman, S. B. V., & Fuqua, C. (2004). Biofilm formation in plant-microbe associations. *Current Opinion in Microbiology*, *7*(6), 602-609. Scopus. https://doi.org/10.1016/j.mib.2004.10.014

Ranf, S., Grimmer, J., Pöschl, Y., Pecher, P., Chinchilla, D., Scheel, D., & Lee, J. (2012). Defense-Related Calcium

Signaling Mutants Uncovered via a Quantitative High-Throughput Screen in Arabidopsis thaliana.

Molecular Plant, *5*(1), 115-130. https://doi.org/10.1093/mp/ssr064

Roux, M., Schwessinger, B., Albrecht, C., Chinchilla, D., Jones, A., Holton, N., Malinovsky, F. G., Tör, M., de Vries, S.,

& Zipfel, C. (2011). The *Arabidopsis* Leucine-Rich Repeat Receptor–Like Kinases BAK1/SERK3 and

BKK1/SERK4 Are Required for Innate Immunity to Hemibiotrophic and Biotrophic Pathogens. *The Plant

Cell*, *23*(6), 2440-2455. https://doi.org/10.1105/tpc.111.084301

Sabarwal, A., Kumar, K., & Singh, R. P. (2018). Hazardous effects of chemical pesticides on human health–Cancer

and other associated disorders. *Environmental Toxicology and Pharmacology*, *63*, 103-114.

https://doi.org/10.1016/j.etap.2018.08.018

Samel, S. A., Wagner, B., Marahiel, M. A., & Essen, L.-O. (2006). The Thioesterase Domain of the Fengycin

Biosynthesis Cluster : A Structural Base for the Macrocyclization of a Non-ribosomal Lipopeptide. *Journal

of Molecular Biology*, *359*(4), 876-889. https://doi.org/10.1016/j.jmb.2006.03.062

Sandor, R., Der, C., Grosjean, K., Anca, I., Noirot, E., Leborgne-Castel, N., Lochman, J., Simon-Plas, F., & Gerbeau-

Pissot, P. (2016). Plasma membrane order and fluidity are diversely triggered by elicitors of plant defence.

Journal of Experimental Botany, *67*(17), 5173-5185. https://doi.org/10.1093/jxb/erw284

Schneider, J., Taraz, K., Budzikiewicz, H., Deleu, M., Thonart, P., & Jacques, P. (1999). The Structure of Two

Fengycins from Bacillus subtilis S499. *Zeitschrift Für Naturforschung C*, *54*(11), 859-866.

https://doi.org/10.1515/znc-1999-1102

Serrão, J. E., Plata-Rueda, A., Martínez, L. C., & Zanuncio, J. C. (2022). Side-effects of pesticides on non-target

insects in agriculture : A mini-review. *The Science of Nature*, *109*(2), 17. https://doi.org/10.1007/s00114-

022-01788-8

Sezgin, E., Levental, I., Mayor, S., & Eggeling, C. (2017). The mystery of membrane organization : Composition,

regulation and roles of lipid rafts. *Nature Reviews Molecular Cell Biology*, *18*(6), Article 6.

https://doi.org/10.1038/nrm.2017.16

Srivastav, A. L. (2020). Chemical fertilizers and pesticides : Role in groundwater contamination. In *Agrochemicals Detection, Treatment and Remediation* (p. 143-159). Elsevier. https://doi.org/10.1016/B978-0-08-103017-2.00006-4

Sussman, M. R., & Harper, J. F. (1989). Molecular biology of the plasma membrane of higher plants. *The Plant Cell*, *1*(10), 953-960. https://doi.org/10.1105/tpc.1.10.953

Théatre, A., Cano-Prieto, C., Bartolini, M., Laurin, Y., Deleu, M., Niehren, J., Fida, T., Gerbinet, S., Alanjary, M., Medema, M. H., Léonard, A., Lins, L., Arabolaza, A., Gramajo, H., Gross, H., & Jacques, P. (2021). The Surfactin-Like Lipopeptides From Bacillus spp. : Natural Biodiversity and Synthetic Biology for a Broader Application Range. *Frontiers in Bioengineering and Biotechnology*, *9*. https://www.frontiersin.org/articles/10.3389/fbioe.2021.623701

Tjellström, H., Hellgren, L. I., Wieslander, Å., & Sandelius, A. S. (2010). Lipid asymmetry in plant plasma membranes : Phosphate deficiency-induced phospholipid replacement is restricted to the cytosolic leaflet. *The FASEB Journal*, *24*(4), 1128-1138. https://doi.org/10.1096/fj.09-139410

Tran, H., Ficke, A., Asiimwe, T., Höfte, M., & Raaijmakers, J. M. (2007). Role of the cyclic lipopeptide massetolide A in biological control of Phytophthora infestans and in colonization of tomato plants by Pseudomonas fluorescens. *The New Phytologist*, *175*(4), 731-742. https://doi.org/10.1111/j.1469-8137.2007.02138.x

Vanittanakom, N., Loeffler, W., Koch, U., & Jung, G. (1986). FENGYCIN-A NOVEL ANTIFUNGAL LIPOPEPTIDE ANTIBIOTIC PRODUCED BY BACILLUS SUBTILIS F-29-3. *The Journal of Antibiotics*, *39*(7), 888-901. https://doi.org/10.7164/antibiotics.39.888

Varma, R., & Mayor, S. (1998). GPI-anchored proteins are organized in submicron domains at the cell surface. *Nature*, *394*(6695), Article 6695. https://doi.org/10.1038/29563

Waszczak, C., Carmody, M., & Kangasjärvi, J. (2018). Reactive Oxygen Species in Plant Signaling. *Annual Review of Plant Biology*, *69*(1), 209-236. https://doi.org/10.1146/annurev-arplant-042817-040322

Williamson, B., Tudzynski, B., Tudzynski, P., & Van Kan, J. A. L. (2007). Botrytis cinerea : The cause of gray mould disease. *Molecular Plant Pathology*, *8*(5), 561-580. https://doi.org/10.1111/j.1364-3703.2007.00417.x

Wójtowicz, K., Czogalla, A., Trombik, T., & Łukaszewicz, M. (2021). Surfactin cyclic lipopeptides change the plasma

   membrane composition and lateral organization in mammalian cells. *Biochimica et Biophysica Acta (BBA) -*

   Biomembranes, *1863*(12), 183730. https://doi.org/10.1016/j.bbamem.2021.183730

Yokoyama, R., Kuki, H., Kuroha, T., & Nishitani, K. (2016). Arabidopsis Regenerating Protoplast : A Powerful Model

   System for Combining the Proteomics of Cell Wall Proteins and the Visualization of Cell Wall Dynamics.

   Proteomes, *4*(4), 34. https://doi.org/10.3390/proteomes4040034

Yu, X., Feng, B., He, P., & Shan, L. (2017). From Chaos to Harmony : Responses and Signaling upon Microbial

   Pattern Recognition. *Annual Review of Phytopathology*, *55*(1), 109-137. https://doi.org/10.1146/annurev-

   phyto-080516-035649

Annexes
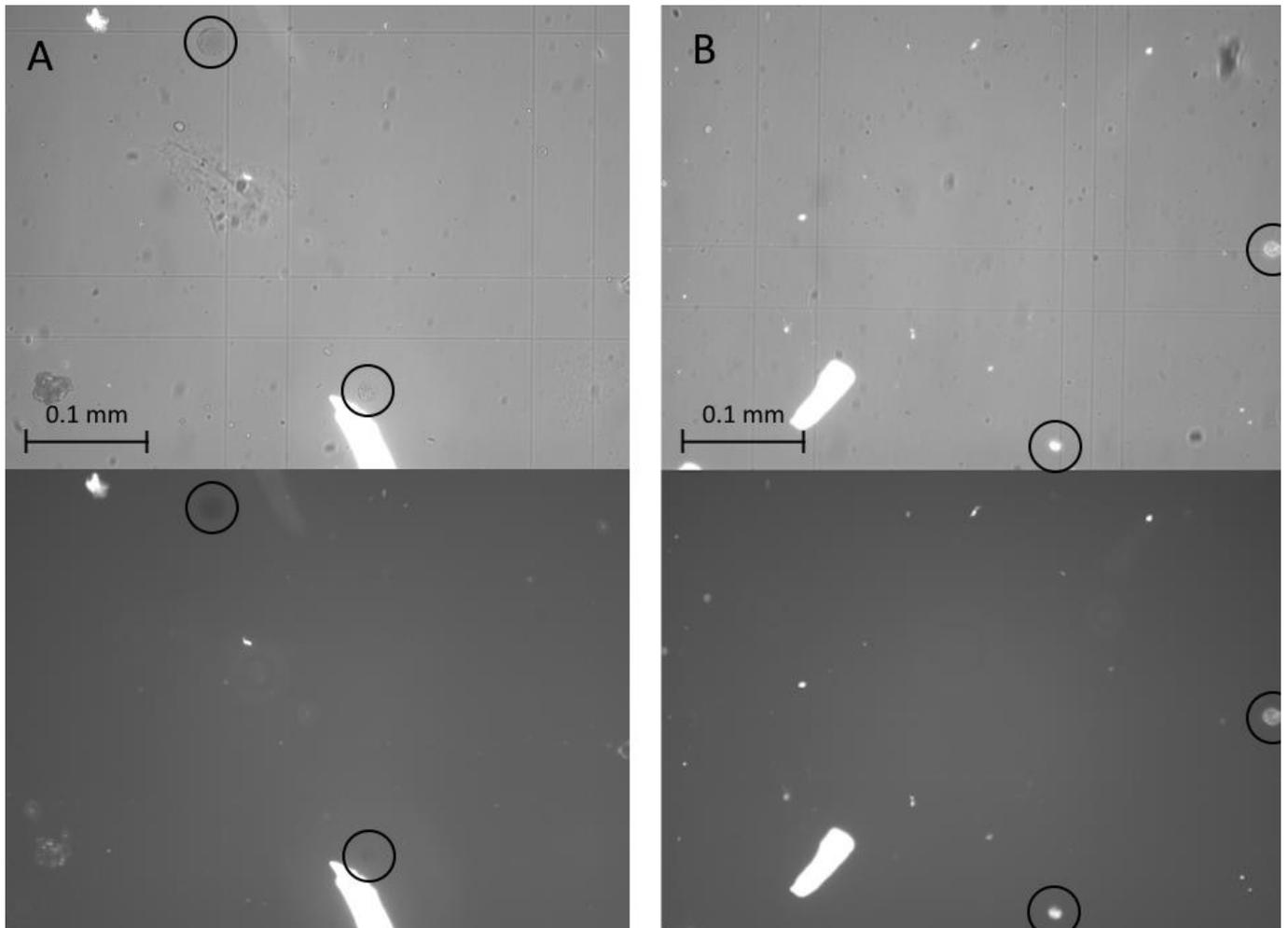
Annex 1 Cell wall regeneration in Brachypodium sylvaticum *protoplasts marked with calcofluor under high (top) and low (bottom) luminosity [A] Freshly isolated protoplasts [B] 1-day-old protoplasts.*
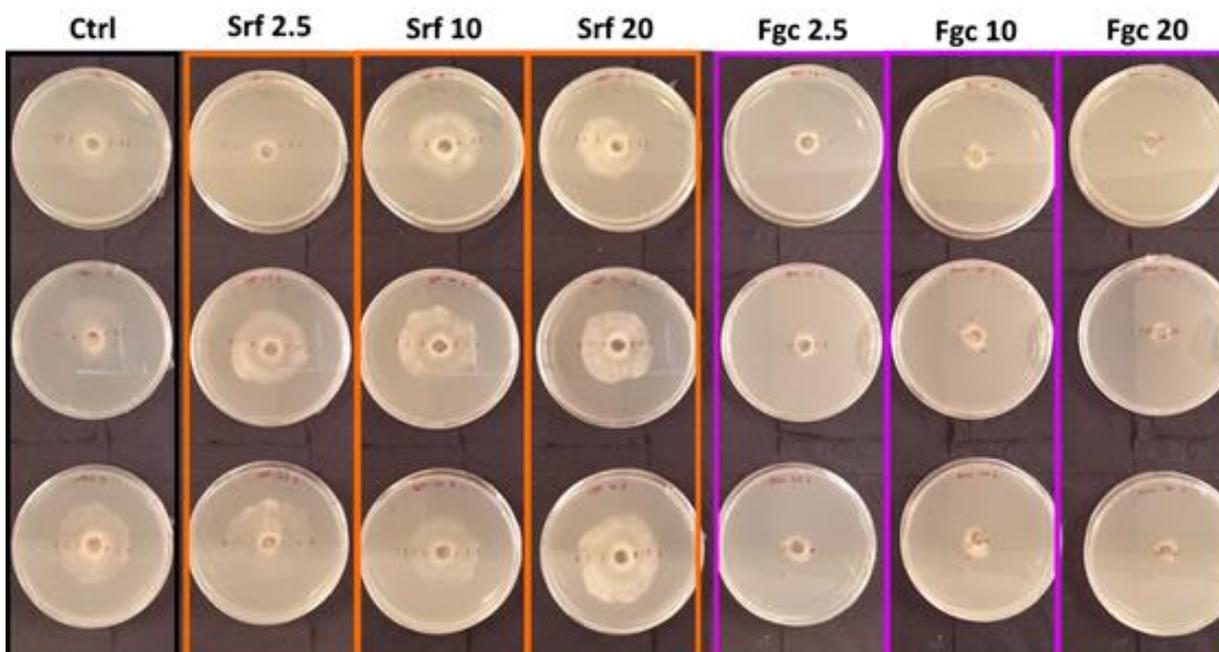

Annex 2 Inhibition of B. cinerea *mycelial growth experiment on PDA plates after 72 hours treatments with 2.5µM, 10µM or 20µM of either surfactin (srf) or fengycin (fgc) diluted in ethanol, control contains ethanol..*

Annex 3 Microplate retrieved after first replicate of the spore germination experiment under protocol N°1.
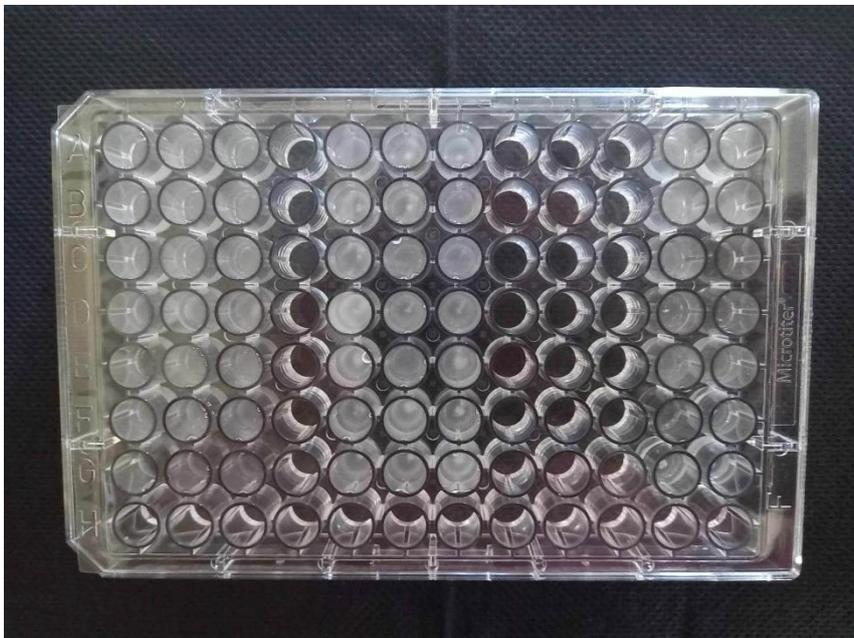
Annex 4 Microplate retrieved after second replicate of the spore germination experiment under protocol N°1.
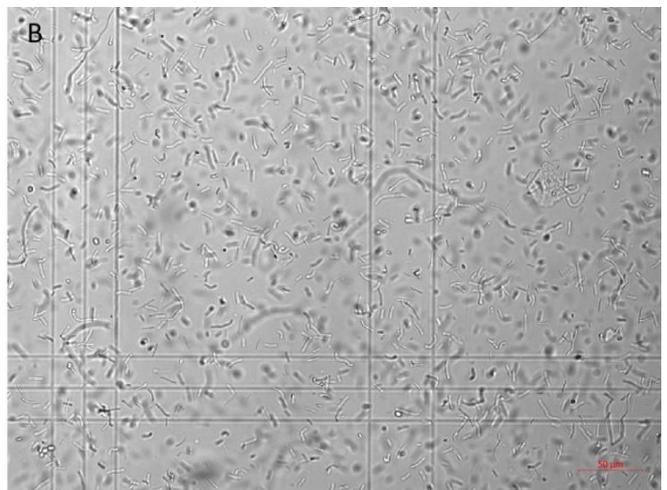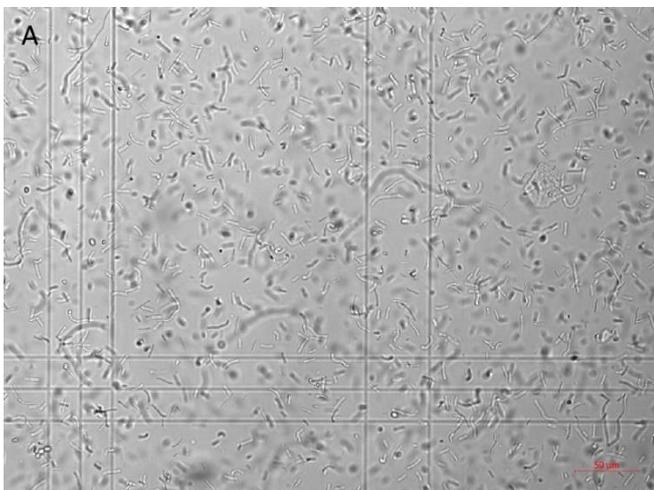
Annex 5 Contamination in the culture medium of [A] 20μM fengycin and [B] 20μM surfactin treated spore suspension of B. cinerea *used in the second protocol of the spore germination inhibition experiment.*